Atomic Layer Deposition

J. Ruud van Ommen, Aristeidis Goulas, Riikka L. Puurunen,

Kirk-Othmer Encyclopedia of Chemical Technology, John Wiley & Sons

First published: 16 September 2021

https://doi.org/10.1002/0471238961.koe00059

Abstract

Atomic layer deposition (ALD) is a gas-phase method to grow layers of solid materials with subnanometer precision. It has been invented independently in the Soviet Union in the 1960s under the name molecular layering, and in the 1970s in Finland under the name atomic layer epitaxy. ALD relies on alternatingly exposing a surface to gaseous reactants - separated by a purge step - that react in a self-terminating manner. This article introduces the fundamentals of the surface chemistry of ideal ALD, including saturating and irreversible reactions, growth per cycle, monolayer concepts relevant to ALD, typical surface reaction mechanisms, saturation-limiting factors, growth modes, area-selective ALD, growth kinetics, and conformality. It also discusses typical deviations from ideal ALD. Over the years, many different ALD process chemistries have been developed. A range of reactor systems is available, depending on the type of substrate and required productivity. ALD is broadly applicable in practice since it couples nanoscale precision with a good scalability and can be used to deposit a large variety of materials. In recent years, the interest in ALD has been growing strongly. The most important sector regarding commercial applications of ALD is currently the semiconductor industry.

ATOMIC LAYER DEPOSITION

1. Introduction

Coating solid objects is typically done to either protect the object or to give it additional functionality. A common method is to cover the object to be coated—also referred to as *substrate*—with a film of a solution or a dispersion and leave it to dry. An example from daily life is painting a surface. Working with a liquid has the advantage that it often has the tendency to form a film: this way a coating with a rather homogeneous thickness can be formed. Such coating has a typical thickness of 10–100 μm.

In the semiconductor industry, there has been a trend to make devices smaller and smaller, following Moore's law (1,2). This also increased the demand for coating techniques yielding thinner films, leading to the increased interest in gas-phase coating techniques. Gas-phase coating has the advantage that much thinner films can be achieved, as surface tension is not playing a role.

There are physical and chemical approaches to gas-phase coating (see Fig. 1). Several physical coating approaches, such as sputtering and molecular beam epitaxy, are line-of-sight techniques: there is a linear flow path of material from source to substrate. This strongly limits the possibility to provide objects with a complex geometry with a conformal coating, that is, a coating that completely follows the contours of an object and has a constant thickness. Chemical coating approaches, with chemical vapor deposition (CVD) as an important example, do not have this problem. In CVD, typically two reactant gases are simultaneously brought into contact with the substrate, leading to the growth of a solid coating at the surface.

However, with further reduction in typical semiconductor dimensions, CVD also becomes too coarse: it shows variation in coating thickness and is not well able to coat deep trenches. A variant of CVD that has drawn more and more attention since about 2000 is *atomic layer deposition* (ALD). With ALD, it is possible to make coatings with a thickness in the nanometer range. Moreover, ALD has unparalleled conformality: the film completely follows the contours of an object and has a constant thickness. By working at the nanoscale, electromagnetic, optical, and chemical effects can be obtained that are differing from those for thicker coatings. Moreover, for such ultrathin films, only small amounts of materials are required, which is an advantage when working with scarce materials.

Dissimilar to most surface coating techniques where the substrate is exposed to the reactants simultaneously, in ALD the substrate to be coated is consecutively exposed to the reactant gases. Typically, two reactants are used, and the sequencing is repeated a number of times (Fig. 2). The substrate is commonly held in a reaction chamber that is kept under vacuum. ALD is normally carried out at elevated temperature: temperatures are often in the range of 120–300°C, but lower or higher temperatures are also used. In the first step, Reactant A—typically a metal atom with ligands—is fed to the reaction chamber. This reactant is bound to certain surface groups of the substrate, such as hydroxyl and oxygen groups, in a self-terminating manner. In the second step, the system is purged by a flow of inert gas or emptied by (further) reducing the pressure. In the third step, Reactant B—typically a nonmetal compound—is fed to the reaction chamber, removing the

DOI: 10.1002/0471238961.koe00059

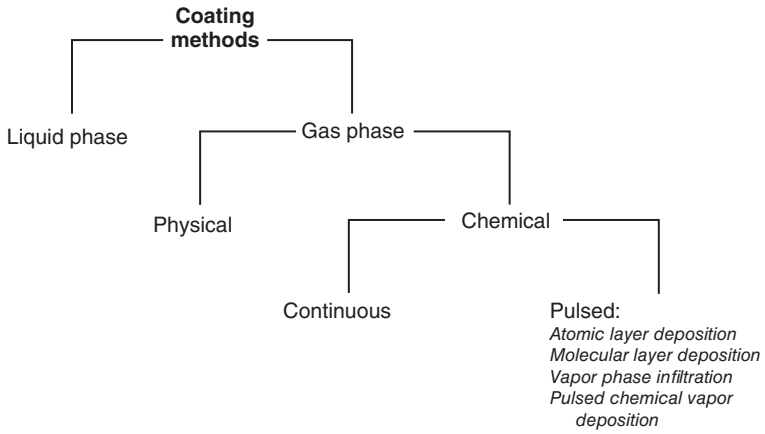

Fig. 1. Schematic overview of the different classes of coating techniques with some examples. Source: van Ommen (2020), Wikimedia Commons, Creative Commons Attribution 4.0 International license.

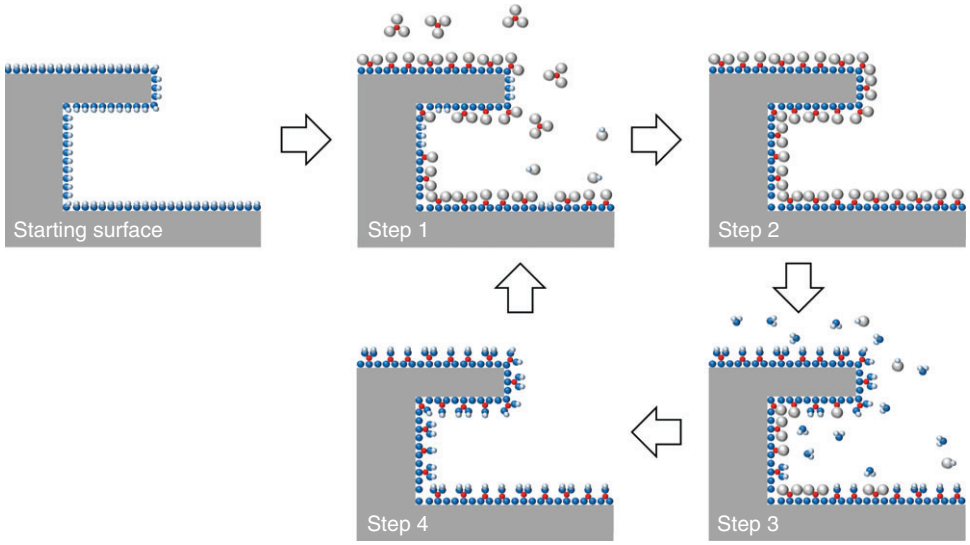

Fig. 2. Schematic illustration of one reaction cycle of the atomic layer deposition (ALD) process. One reaction cycle consists of four steps. Step 1 is the reactive adsorption of Reactant A, Step 2 is a purge or evacuation step, Step 3 is the reactive adsorption of Reactant B, and Step 4 is a purge or evacuation step. Source: Adapted from Goulas and co-workers (2020), Wikimedia Commons, Creative Commons Attribution 4.0 International license.

remaining ligands from the surface and repopulating the surface with functional groups. Finally, in the fourth step, the system is purged or evacuated again. With these four steps, a single ALD cycle is completed, and less than one monolayer of the material has been deposited. After this, the ALD cycle can be carried out again starting from Step 1. This repetition of the four steps is rerun until the required amount of material has been grown on the surface. This can be in the form of a film, typically with a very homogeneous thickness. Several combinations of substrate and grown materials do not yield a film but show a so-called island growth:

islands or nanoclusters are formed at the surface. The materials grown with ALD typically have an amorphous or a polycrystalline nature (3).

The term "ALD" is reserved for the growth of inorganic coatings via sequencing of gas-phase reactants. When the reactants are purely organic precursors, yielding an organic coating, it is called *molecular layer deposition* (MLD) (4). It is also possible to have a hybrid approach, for example, when Reactant A is a metal precursor, and Reactant B is an organic molecule. This yields a coating that contains both metal atoms and organic bonds. Some people also call this MLD, while others refer to it as hybrid ALD/MLD (5,6). Both MLD and hybrid ALD/MLD are outside the scope of this article. Neither *pulsed CVD* (a hybrid between simultaneous CVD and ALD) (7) nor *vapor-phase infiltration* (in which reactants do not react on the substrate surface but diffuse into it) (8) will be treated. In the literature, liquid-phase equivalents of ALD have been proposed (9). This can be advantageous, for example, when working with reactants with limited stability. However, this emergent field is also not further included: normally, the term ALD only refers to gas-phase operation.

ALD is known under several other names, such as *molecular layering* (ML), *atomic layer epitaxy* (ALE), and *atomic layer CVD*. The origin of some of these names will be covered in more detail in the section Early History. In the remainder of this article, the nowadays universally used name "ALD" will be used, although one could argue that material is rather grown than deposited on the surface, and that per cycle subatomic layers instead of atomic layers are grown. In the following sections, the history and fundamentals of ALD will be discussed, and the applied chemistry and equipment will be briefly described, alongside some commercial applications. For a more detailed overview of the research in this field, please consult the many reviews of the field such as References (5,10–12); for a longer list of reviews, see Reference (13).

2. Early History

This section focuses on the first decades of the invention and development of ALD, since ALD was invented independently twice. After around 2000, ALD became widely picked up around the world, and describing its further development would take a much longer text. Some of those developments are, however, covered in Section 6.

ALD has been invented independently in the Soviet Union in the 1960s under the name *molecular layering* (ML) (14) and in the 1970s in Finland under the name *atomic layer epitaxy* (ALE) (14–17). The inventors of ML were Valentin Borisovich Aleskovskii and his student Stanislav Ivanovich Koltsov. They worked at what is now called the St. Petersburg State Technological Institute and were educated in chemistry and chemical engineering. In the 1950s, Aleskovskii had proposed the "*framework hypothesis*," which stated that chemical bonds in the bulk of a solid differ from those at the surface, and thus surface reactions have a different nature than reactions with the bulk material (14). The development of ML was a next step in this, making use of the different nature of surface reactions; the name ML (молекулярное наслаивание) was coined in 1965 (16). Aleskovskii and Koltsov started their experiments with metal chlorides and water as reactants

and porous silica as the substrate. The principles of ML were summarized in the doctoral thesis of Koltsov in 1971 (18). A large number of PhD students devoted their work to ML, especially in the 1970s and 1980s. An extensive part of the work was dedicated to depositing materials such as vanadium, chromium, and germanium compounds on silica gel and single crystal silicon. Typical applications considered first were sorbents, catalysts, and rubber fillers; later on, the importance for microelectronics was also realized (14). The work was picked up in, for example, the East Germany and Bulgaria. However, Soviet researchers hardly published in international journals in those days, and the technique remained unnoticed in the Western world for a long time (14).

In 1974, the Finnish inventor–researcher Tuomo Suntola, trained in electronics engineering and semiconductor physics, was hired by the company Instrumentarium Oy in Espoo (Finland) with the goal "to invent something" (17). Novel flat display technology became his focus. For electroluminescent flat panel displays, the then available film deposition techniques did not yield a high enough quality. Therefore, Suntola thought of a way to have more control of the order in the film: he developed ALE of ZnS, with vaporized zinc and sulfur as the reactants. The sources for the elemental reactants were heated to obtain the desired vapor pressures (17). In the second half of 1974, the first experiments were carried out, and a patent was filed (15). Suntola had to attend hearings to defend the patent in several countries, including the Soviet Union. No critical prior art was presented by the patent examiners (17). In the subsequent years, it was found that using $ZnCl_2$ and H_2S made the production of ZnS easier and better suited for scale-up. Subsequently, the ALE of other materials was also investigated. The reactor and process for making electroluminescent displays were patented in 1979 (19). In 1983, the pilot production of thin-film electroluminescent (TFEL) displays started (see Section 6). In 1987, Suntola moved to the Finnish national oil company Neste and started the subsidiary Microchemistry focusing on ALE. In 1999, Microchemistry was sold to ASM (17). For the development of ALD, Suntola received the European SEMI award in 2004 and the Millennium Technology Prize in 2018.

In the 1980s, researchers across Finland, and also in the rest of Europe, North-America, and Japan, picked up Suntola's work and started to work on ALD (then still called ALE) (20). In 1984, the First Symposium on Atomic Layer Epitaxy took place in Espoo, Finland (21). The same city hosted the First International Conference on ALE (ALE-1) in June 1990 (22). At this conference, the name "ALD" was proposed as an alternative to ALE in analogy with CVD (23), but it took a decade before this name was generally accepted (24). ALE-1 was also attended by Victor Drozd, a Russian ALD researcher (17,25). Suntola was invited to visit Leningrad (Saint Petersburg); he went there in August 1990. Aleskovskii presented his work dealing with oxide layer build-up based on saturated surface reactions, the same as in the ALE process. The discussion confirmed that the essence of ALE had been independently discovered by the Aleskovskii group (17). Although a review paper by Aarik et al. (26) in 1990 discussed both ML and ALE, the literature on ML received little attention from researchers in the Western World in the 1990s and 2000s. More recently, it started to attract more attention (10,27,28). Around 2000, the commercial importance of ALD strongly increased as it entered the industry for hard disk heads and memory chips; this will be discussed more in detail in Section 6.

3. Fundamentals

3.1. Ideal ALD: Saturating and Irreversible Reactions. Growth of thin solid films by ALD is based on the repeated alternating, well-separated, and self-terminating reactions of typically two gas-phase compounds, here called *Reactant A* and *Reactant B*, with the surface of a solid material (ABAB … sequence). The solid material is often called a *substrate*. The gas-phase compounds are most often multielement molecules and sometimes single elements or atoms. At room temperature, the reactants can be solids, liquids, or gases; at ALD temperature, they must necessarily be gaseous (more on reactants in Section 4). In energy-enhanced ALD such as plasma-enhanced atomic layer deposition (PEALD, also called plasma-assisted ALD), other types of gas-phase species can be present, for example, radicals; for the details of such processes, the reader is guided to specialized reviews (29,30). The gas-phase species undergo reactions with the solid surface, leading to enrichment of adsorbed species on the surface, which is often accompanied by the release of *gaseous reaction by-products*. The gaseous reaction by-products are preferably inert and do not react with the surface. Figure 2 gives a schematic illustration of an ALD reaction cycle inspired by the characteristics of the archetypical trimethylaluminium (TMA)–water ALD process.

In each ALD reaction step, gaseous species interact with the surface in an adsorption process where chemical bonds are being formed and optionally broken. These reactive adsorption steps classify as *chemical adsorption* or, in short, *chemisorption*. ALD fundamentally relies on the condition that the chemisorption steps are allowed to saturate, to go to completion—forming a monomolecular layer of the chemisorbed species by definition (31)—before proceeding to the next steps, which are the removal of excess reactants by purge/evacuation and the next chemisorption step. ALD also relies on the condition that the chemisorbed species remain on the surface during the purge/evacuation step: the chemisorption is *irreversible*. In ideal ALD, *physical adsorption* (in short, *physisorption*) is excluded, as it would not saturate at a monomolecular layer and it is, by its nature, *reversible*. An illustration on how the amount of adsorbed species changes with time during the reaction and purge/evacuation step in ALD (Steps 1&2 or 3&4 in Fig. 2) is shown in Figure 3**a**. Figure 3**b–g** illustrates the typical deviations from characteristic ALD behavior by reactions that are either not saturating or not irreversible.

A more detailed illustration of the characteristic changes on the surface during ALD is shown in Figure 4. Figure 4**a** shows the ALD cycles divided into four characteristic steps and the surface termination resulting from the reactions of Reactant A and Reactant B. Figure 4**b** presents how the reactants are pulsed into the reaction chamber, with their partial pressures represented by a step function, with inert gas acting as a carrier and purge gas. In this simplified example, the total pressure stays constant during the pulsing; such is not necessarily the case in practice (32). Figure 4**c** illustrates how the surface coverages of adsorbed species from Reactant A and Reactant B alternate on the surface during the pulsing; here, the characteristics of Figure 3**a** are repeated. Finally, Figure 4**d** shows the mass adsorbed as function of time, as well as the change in mass with time. In this example, the mass *increases* in the reactions of Reactant A and B. In some ALD processes, the mass *decreases* in a reaction step, when heavier surface species get

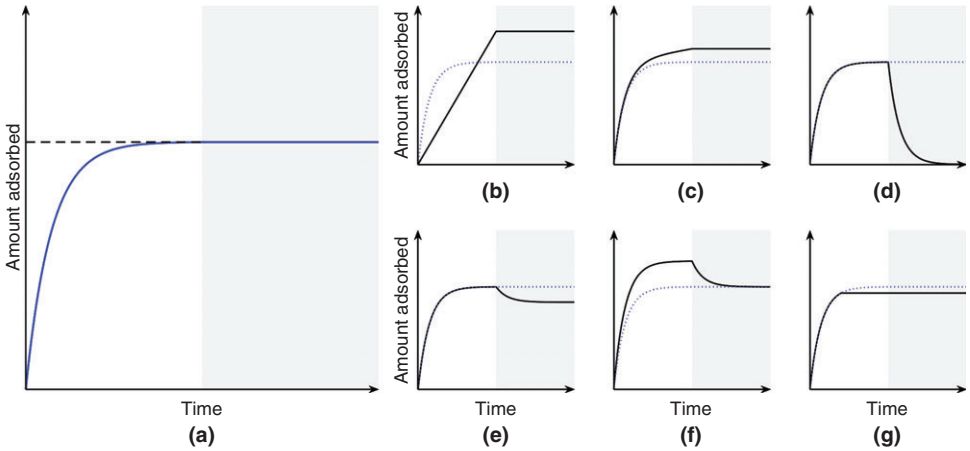

Fig. 3. Illustration of various time dependencies of the amount adsorbed versus time in gas–solid reactions during reactant exposure (white background) and a following purge/evacuation (gray background): (**a**) saturating, irreversible reaction (chemisorption); (**b**) nonsaturating continuous reaction; (**c**) a combination of saturating, irreversible reaction and a continuous reaction component; (**d**) fully reversible adsorption (either chemisorption or physisorption); (**e**) partly reversible chemisorption; (**f**) a combination of saturating, irreversible chemisorption and reversible physisorption; and (**g**) saturating, irreversible reaction where reactant feed is stopped before saturation occurs. Panel (**a**) corresponds to *ideal ALD*. Source: Puurunen and van Ommen (2020), Wikimedia Commons, Creative Commons Attribution 4.0 International license.

replaced with lighter ones. From Figure 4**d** it is evident that ALD is a transient nonequilibrium process, with the amount of material adsorbed on the surface constantly changing with time. Thus, no *pseudo steady state* with a constant nonzero *growth rate* (with time), characteristic for most CVD processes, is obtained in ALD.

Once the irreversible reaction has reached saturation and the chemisorbed monolayer has formed, parameters such as partial pressure of the reactant and time of the reaction step should not play any role. Ideally, the amount and type of adsorbed species are defined by the reactant, the surface, and the reaction temperature.

3.2. Growth Per Cycle (GPC) in ALD. The amount of material added onto the surface in one ALD reaction cycle is called the *growth per cycle* (GPC). Often, GPC is taken to be synonymous with thickness per cycle, although more specific expressions can be used, such as thickness per cycle (unit, eg, nm) and mass gain per cycle (unit, eg, ng/m^2). The GPC does not tell *how fast* an ALD process is; it tells *how much* material is grown in one ALD reaction cycle. The GPC and the digital control of the amount deposited by counting the number of cycles, rather than by adjusting the deposition time, is among the well-known benefits of ALD.

In the literature, sometimes, the term “growth rate (per cycle)” is used instead of GPC. Because the amount of material added in an ALD cycle is not a rate as in chemical kinetics (quantity per time unit), the term “growth rate (per cycle)” is misleading, and the authors of this article discourage the use of this term.

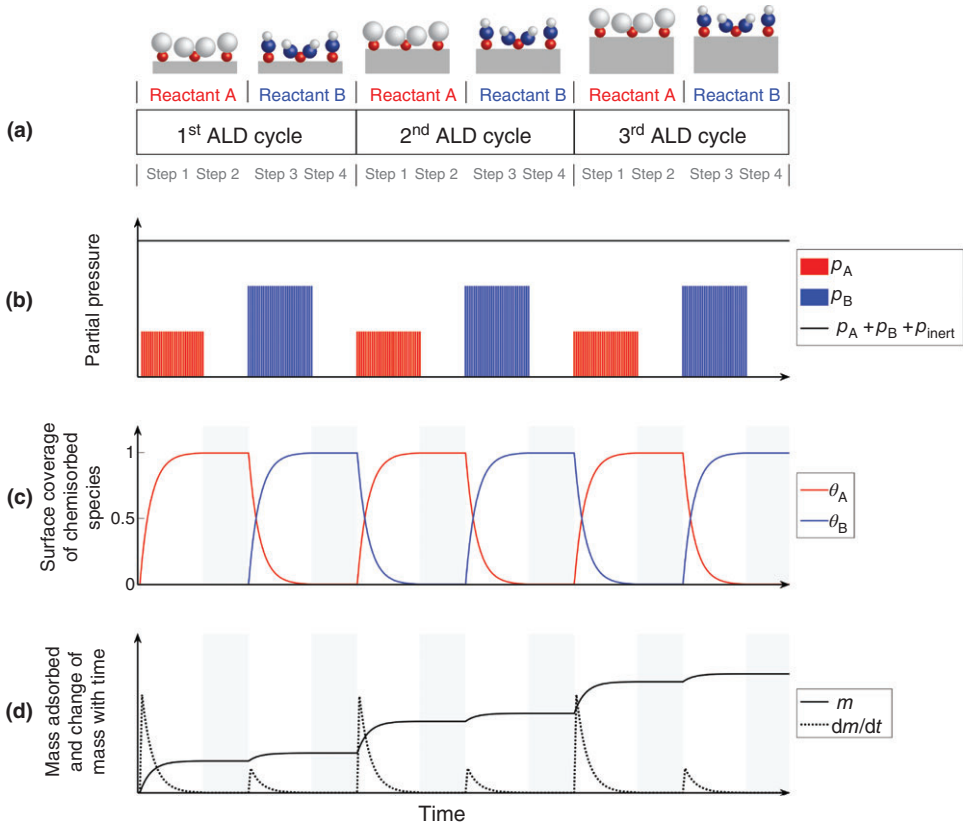

Fig. 4. Schematic illustration of changes with time during three ALD reaction cycles (white background: reaction step; gray background: purge/evacuation): (**a**) division of an ALD cycle in four steps, with surface terminations after Reactants A and B shown; (**b**) partial pressures of Reactants A and B and inert carrier gas; (**c**) surface coverage of chemisorbed species from Reactants A and B (after first reaction cycle, Step 1, $\theta_A + \theta_B = 1$); (**d**) mass adsorbed and change in mass adsorbed with time. Source: Puurunen and co-workers (2020), Wikimedia Commons, Creative Commons Attribution 4.0 International license.

When an ALD reaction cycle is repeated and the material grows on itself, GPC is typically the same in each ALD cycle. The ALD growth is said to be in the *constant regime* or, synonymously, in the *linear regime*. Figure 5**a.1** illustrates a constant GPC with cycles, and Figure 5**b** the corresponding linear growth curve with cycles. In the beginning of the ALD growth, when the substrate material is necessarily exposed on the surface, the GPC often varies with cycles. Compared to the linear growth regime, depending on the amount and reactivity of adsorption sites on the surface, the GPC in the first cycle(s) can then be *higher* (Fig. 5**a.2**) or *lower* (Fig. 5**a.3**, **a.4**). The growth is then called *substrate-enhanced* or *substrate-inhibited growth*, respectively. Substrate-inhibited growth has been further divided into two characteristic categories: Type 1 and Type 2 (10). In Type 1 substrate-inhibited growth, typically a few ALD reaction cycles are sufficient to increase to a constant GPC. In Type 2 substrate-inhibited growth, it may take tens or hundreds of cycles for the growth to reach linearity. This type of growth

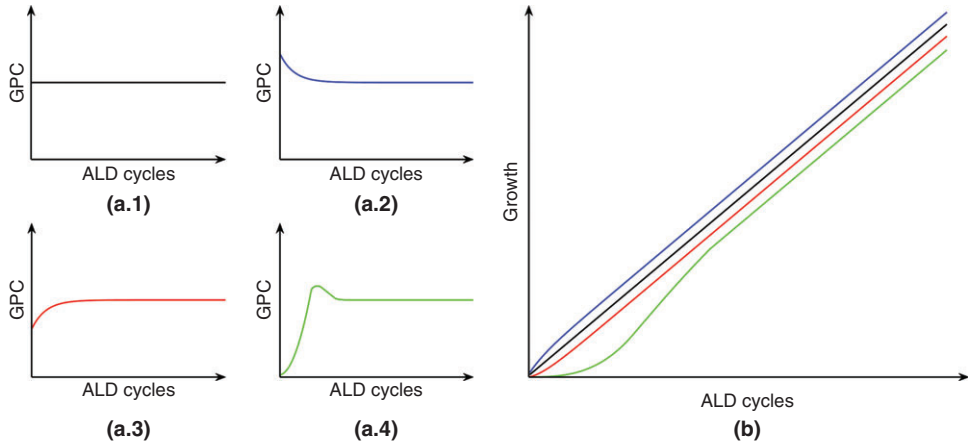

Fig. 5. Illustration of different characteristic ways the GPC can vary with cycles: (**a.1**) constant GPC; (**a.2**) substrate-enhanced growth, with GPC that is higher in the beginning; (**a.3**) Type 1 substrate-inhibited growth, where GPC is lower in the beginning; and (**a.4**) Type 2 substrate-inhibited growth, where GPC is small in the beginning, increases often with a quadratic dependency on the cycle number, and later levels off to a constant value, optionally after going through a maximum. The characteristic shape of the *growth curve*, resulting from the growth in panels (**a.1**)–(**a.4**), is illustrated in panel (**b**). Classification as in Ref. 10. Source: Puurunen and van Ommen (2020), Wikimedia Commons, Creative Commons Attribution 4.0 International license.

is typical for surfaces with low amounts of reactive sites (eg, growth of oxides on defect sites of hydrogen-terminated silicon). In such cases, growth takes place on islands or particles that grow and coalesce, and the GPC often has a *quadratic* ($\propto n^2$) dependency on the cycles (33). Type 2 substrate-inhibited growth can be exploited in area-selective atomic layer deposition (ASALD), see Section 3.7.

Deviations from constant GPC with cycles at higher cycle numbers, when the material grows on itself, can also take place, when seen from top (perpendicular to the surface). For example, when the film grows polycrystalline and the GPC value differs on the exposed facets, the dominance of one fast-growing facet may increase the observed average GPC. Also, changes in surface roughness cause changes in the GPC (34).

In ALD, based on saturating, irreversible reactions, the GPC is defined by the reactants, the surface, and the temperature at which the chemisorption process takes place. In the literature, one often encounters the assumption that the GPC should remain constant with increasing temperature (in the so-called ALD temperature window or ALD window, in short), where GPC is also often misleadingly assumed to be ideally equivalent to a "full (bulk) monolayer", see Section 3.3. However, it is evident that the reactivity of the reactant as well as the characteristics of the surface (eg, the areal number density of a particular type of reactive sites, nm^{-2}) both can be functions of temperature (10,35). Consequently, with ALD conditions fulfilled, there can be various trends in the GPC versus temperature in ALD, as illustrated in Figure 6: the GPC can stay constant, increase or decrease (gradually or in steps), or go through a maximum or a minimum.

3.3. Three Different Monolayer Concepts Relevant to ALD. In the scientific ALD literature, a (mis)conception has spread widely that, somehow, ALD

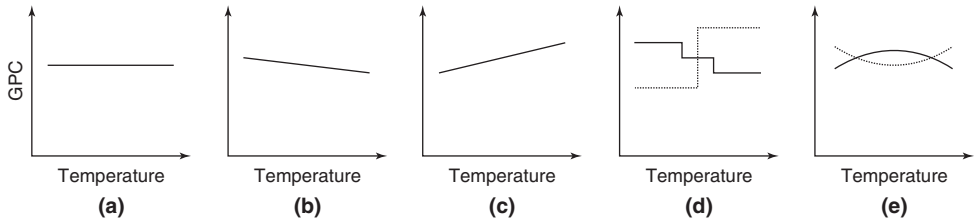

Fig. 6. Illustration of the ways the GPC can vary with temperature: (**a**) be constant, (**b**) decrease, (**c**) increase, (**d**) decrease or increase in steps, or (**e**) go through a maximum or a minimum. Source: Puurunen and van Ommen (2020), Wikimedia Commons, Creative Commons Attribution 4.0 International license.

should result in what is called "*full monolayer growth*." Here, "monolayer" refers to the bulk of the material being grown. This misconception is repeated in many schematic cartoons illustrating the ALD process and review articles, despite the fact that it has been noticed since the early days of ALD that growing a *fraction* of a monolayer of the bulk material is typical for ALD processes, and "full monolayer growth" is extremely rare. For example, the ALD process from elemental Zn and S reactants results in a third of a monolayer of ZnS per cycle (17). So does also the archetypical ALD process from TMA and water, with a GPC of roughly a third of a monolayer of Al_2O_3, which decreases with increasing temperature (10). In an attempt to correct the widespread misconception, the schematic illustration of ALD of this article (Fig. 2) is consistent with the growth of approximately one-third of a monolayer of the bulk material.

One reason behind the persistent misconception of "full monolayer growth" in ALD may be the fact that the term *monolayer* (ie, *monomolecular layer*) can have several different conceptual meanings. There are three such monolayer concepts related to ALD, which can be mixed up. This section tries to clarify the meanings of three fundamentally different monolayers relevant to ALD.

The three fundamentally different monolayers relevant to ALD are illustrated in Figure 7. Figure 7**a** shows a *chemisorbed monolayer*, that is, a

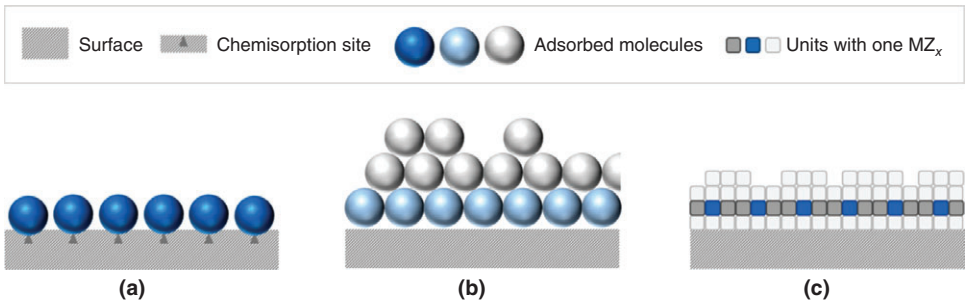

Fig. 7. Schematic side-view illustration of three fundamentally different monolayers relevant to ALD: (**a**) chemisorbed monolayer, which is the basis of ALD growth; (**b**) physisorbed monolayer, with adsorbed species closely packed and with multilayers adsorbed on top, serving as a useful reference point for theoretical maximum GPC ALD; and (**c**) a bulk monolayer of the ALD-grown material, with a GPC of one-third of the bulk monolayer illustrated with blue squares. Source: Puurunen (2020), Wikimedia Commons, Creative Commons Attribution 4.0 International license.

monomolecular layer of chemisorbed species. A monolayer is by definition formed in chemisorption after saturation has been attained (31). In this simple illustration, all adsorption sites are illustrated as equal; in reality, there may naturally be various types of adsorption sites on the surface. Apart from ALD, chemisorbed monolayers are used, for example, to probe the active metal surface area of heterogeneous catalysts (often after dissociative chemisorption of hydrogen). Figure 7**b** illustrates a *physisorbed close-packed monolayer,* with physisorbed multilayers on top of it. A physisorbed close-packed monolayer can serve as a useful theoretical maximum reference point for considering the number of adsorbed molecule fragments or ligands of a given size that can fit into a unit surface area of a substrate (36). Apart from ALD, physisorbed monolayers (eg, with nitrogen as a probe molecule) are used to assess the surface area of solid materials by the Brunauer–Emmett–Teller method. Figure 7**c** presents an average bulk monolayer of the ALD-grown material. Here, each cube contains one average unit of the MZ_x material. For any material, one can calculate for an average bulk monolayer the thickness $\bar{h}^{\mathrm{ml}}$ (nm) and areal number density of metal M $\bar{c}_{\mathrm{M}}^{\mathrm{ml}}$ (nm^{-2}) (ie, the number of M atoms per unit surface area). For the calculation, the mass density ρ of the MZ_x material and the molar mass M of the MZ_x unit are needed (36): $\bar{h}^{\mathrm{ml}} = (M/\rho\, N_{\mathrm{A}})^{1/3}$ and $\bar{c}_{\mathrm{M}}^{\mathrm{ml}} = (\bar{h}^{\mathrm{ml}})^{-2} = (\rho\, N_{\mathrm{A}}/M)^{2/3}$ (N_{A} is Avogadro's constant). If the crystallographic orientation of the material being grown is known, the interatomic spacing can give a more accurate value for the bulk monolayer thickness of the material.

3.4. Surface Reaction Mechanisms. Reaction mechanisms that take place during ALD are typically classified into three categories: *ligand-exchange reaction*, *associative adsorption*, and *dissociative adsorption* (10,37,38). Yet, a distinct type of reaction, deserving its own category, is *combustion* that takes place with oxidizing reactants. The four categories of reaction mechanisms are described in more detail below. Besides the four mechanisms discussed here, additional mechanisms may play a role.

For the description, it is assumed that Reactant A is a metal reactant with the formula ML_n. The ALD-grown material is denoted with MZ_x, a surface nonmetal atom as ||Z, and a surface nonmetal (or metal) atom with a reactive group attached as ||Z–a (or ||M–a).

Irrespective of the detailed surface reaction mechanism that leads to the attachment of surface species in the reaction of Reactant A, the ALD reaction will attain saturation after the chemisorbed monolayer (Fig. 7**a**) has formed. At saturation, the adsorbed species added onto the surface in the ML_n reaction are described by an average stoichiometry ML_z.

Ligand-exchange reaction is the most often considered reaction mechanism in ALD. Sometimes, this mechanism is in short referred to as *ligand-exchange* or just *exchange reaction*.

Here, the ML_n compound reacts with a surface site ||Z–a that readily combines with the ligand, creating a volatile by-product compound aL (g), leaving behind ||Z–ML_{n-1} as adsorbed species on the surface, as illustrated in Figure 8**a**. Typically, the oxidation state of the elements does not change in this process. If there are more suitable neighboring ||Z–a sites, the process may be repeated, and more by-product molecules are released in the gas phase, as illustrated

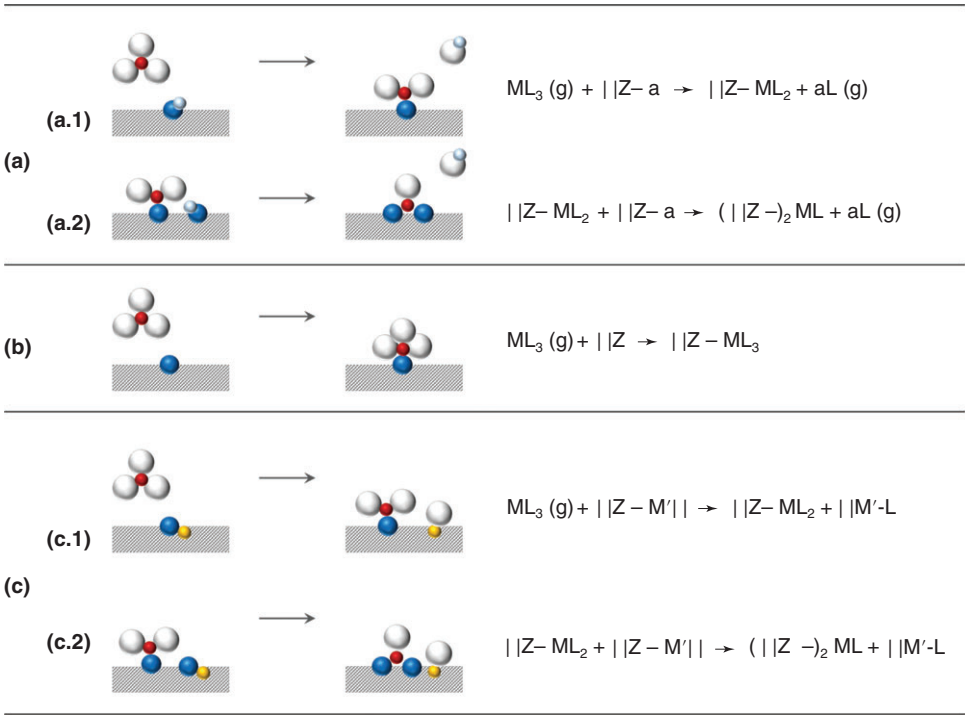

Fig. 8. Illustration of three typical classes of surface reaction mechanisms in ALD for molecule ML_n (here, $n = 3$): (**a**) *ligand-exchange reaction*, where a gaseous reaction by-product aL is released; (**b**) *associative adsorption*, where a bond is formed between a surface site and the molecule; and (**c**) *dissociative adsorption*, where all parts of the ML_n molecule are bonded to the surface in a process where bonds are broken and made. Ligand-exchange reaction and dissociative reaction can take place further between an adsorbed species and a neighboring surface site (**a.2**, **c.2**). Source: Puurunen (2020), Wikimedia Commons, Creative Commons Attribution-Share Alike 4.0 International license.

in Figure 8**a.2**. After multiple repetitions of the ligand-exchange reaction, the adsorbed species on the surface have an average stoichiometry z in $(\|Z–)_{n-z}ML_z$, where $z < n$. The occurrence of ligand-exchange reaction can be inferred by measuring the average stoichiometry of the surface ML_z species ($[L]/[M] = z$) ratio as well as analyzing the gas-phase species inside or flowing out from the ALD reactor.

Most often, ligand exchange is hydrogen mediated, meaning that ||Z–a corresponds to ||Z–H. For example, for the TMA-water process, the generation of methane (CH_4) is observed due to the ligand-exchange reaction with ||O–H, and the average [L]/[M] stoichiometry on the surface is decreased from three to two or below (10). In processes based on metal chlorides (eg, $AlCl_3$, $TiCl_4$, and $HfCl_4$) and water to grow, the corresponding metal oxide, HCl is observed as a by-product. The release of a gaseous by-product and its continuous removal by an inert purge helps to make the reaction in practice irreversible. Other possibilities exist for mediators of ligand exchange in addition to hydrogen; for more details, see Reference (37).

Associative adsorption, or *association* in short, is another class of chemisorption mechanism relevant to ALD. Association, illustrated in Figure 8**b**,

can take place when the metal cation in Reactant A or on the surface is electron deficient (eg, a transition metal has less than 18 valence electrons), and it can accept an electron pair, for example, from oxygen, nitrogen, or sulfur anions through a Lewis acid–base adduct formation. In such process, molecular adsorption of Reactant A (ML_n) takes place through ||Z–M interaction, or Reactant B through ||M–Z interaction, where Z is a nonmetal in Reactant B. A coordination bond is formed between a surface element and an element in the reactant. The adsorption is site specific and necessarily saturates at a monolayer (as opposed to physical adsorption, which does not saturate). When associative adsorption (chemisorption) has occurred, the [L]/[M] stoichiometry on the surface equals that in Reactant A, that is, n for ML_n. No by-products are released into the gas phase.

A classic example of an ALD process where associative adsorption takes place is the $ZnCl_2$–H_2S process to grow ZnS. In the reaction of $ZnCl_2$ on a sulfur-terminated surface, molecular chemisorption (association) of $ZnCl_2$ via sulfur–zinc bond formation was concluded based on both *in situ* mass spectrometry measurements and quantum chemical calculations (20). Associative adsorption (whether chemisorption or physisorption) is also often considered as the first elemental step in quantum chemical investigations of surface reactions in ALD.

Dissociative adsorption, or *dissociation* in short, is the third generic class of chemisorption mechanisms in ALD. In dissociation, illustrated in Figure 8**c**, a ligand is transferred from the ML_n molecule to a surface cation, giving ||M′–L on the surface at the same time as surface-bound ||Z–ML_{n-1} is formed. All fragments of ML_n are thus chemically bonded to the surface. Similarly, as in ligand-exchange reaction, the ||Z–ML_{n-1} species can potentially undergo more reactions on the surface to dissociate more ligand and make $(||Z–)_2$ ML_{n-2} and another ||M′–L, and so on. The summed average [L]/[M] stoichiometry of all surface species equals n, similar as in associative adsorption; also, no by-products are released into the gas phase. Therefore, one cannot discern whether association or dissociation takes place merely by examining the [L]/[M] ratio; more detailed surface analysis is needed.

One classical example of dissociative adsorption as a chemisorption mechanism is the reaction of TMA on silicon dioxide. Here, dissociation of siloxane bridges ||Si–O|| is evidenced, for example, by infrared or nuclear magnetic resonance spectroscopy by the formation of silicon-bonded methyl (Me) groups ||Si–Me in addition to aluminum-bonded methyl groups ||O–$AlMe_x$ (10,39). It is likely that the dissociative mechanism also takes place on alumina that has a low number of hydroxyl groups (10). A more recent characteristic example is the dissociation of noble metal reactants on a metallic surface, for example, $Ru(EtCp)_2$ giving ||Ru–CpEt and ||–CpEt (37,40).

Combustion (oxidation) takes place during the reaction of oxidizing nonmetal reactants (Reactant B) and sometimes due to surface (and subsurface) oxygen during the reaction of the metal reactant (Reactant A). Combustion typically occurs when oxygen or ozone (or oxygen plasma) is used as Reactant B. Organic ligands L of the adsorbed species ||–ML_z are eliminated in this way. In full combustion, the gaseous reaction products are the total oxidation products, that is, CO_2 and water; when the supply of oxygen is limited, partial oxidation products may also form.

Noble-metal ALD processes combined with oxidizing Reactant B are a typical class of ALD processes based on combustion reactions. Noble metals often catalyze combustion. Despite the use of oxidizing agents, metallic films can often be grown because the nature of noble metals favors reduction (41). Another typical class of examples is ALD processes relying on metal-β-diketonate compounds. Water typically is unable to remove the β-diketonate ligands through ligand exchange, and therefore, combustion reactions are required for the ALD process to occur.

3.5. Saturation-Determining Factors. Two possibilities are typically considered as the *saturation-determining factor* in ALD, depending on the reactant and the surface: *running out of reactive sites* and *steric hindrance*. These two factors can play a role separately or simultaneously.

When the surface runs out of reactive sites, saturation occurs because there are no sites for the incoming reactant to react with, even though there is space for the reactant to reach the surface. Running out of reactive sites as saturation-determining factor is illustrated in Figure 9**a**, using a ligand-exchange reaction of a metal reactant ML_n with surface sites of type ||Z–a as an example. One real example, where running out of reactive sites has been concluded to be the saturation-determining factor, is the $HfCl_4$ reaction (to grow hafnium oxide with H_2O) with silicon dioxide surfaces with a low amount of hydroxyl groups (||O–H). Here, the number of ||O–H groups limits the reaction, and the GPC as areal number density of Hf atoms (Hf/nm^2) can be used as a probe for the number of OH groups on the surface before the reaction (42).

When steric hindrance determines saturation, the surface gets covered with ligands, which physically prevent further access to the surface and the further adsorption. In other words, the bulky nature of the ligands makes no space for further reactions to occur. Steric hindrance as a saturation-determining factor

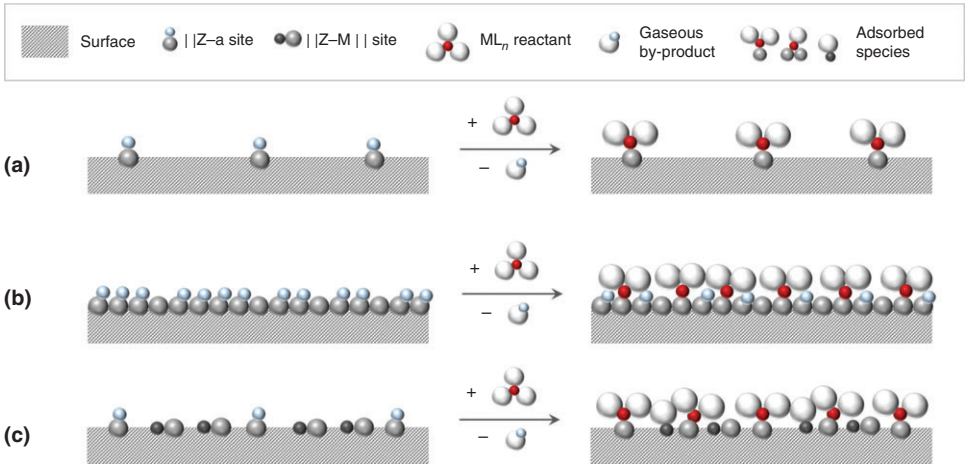

Fig. 9. Illustration of different saturation-determining factors in ALD: (**a**) running out of reactive sites causes saturation; (**b**) steric hindrance causes saturation in ligand-exchange reaction with one ||Z–a group, with reactive sites ||Z–a capable of ligand exchange remaining under the ligand shroud; and (**c**) combination of running out of reactive sites of type ||Z–a and steric hindrance, for a reactant able to react (*1*) via ligand exchange with one ||Z–a group and (*2*) dissociative adsorption onto ||M–Z|| sites. Source: Puurunen and van Ommen (2020), Wikimedia Commons, Creative Commons Attribution 4.0 International license.

is illustrated in Figure 9**b**,**c**. Depending on the surface reaction mechanisms involved, there may remain reactive sites such as ||Z–a on the surface under the ligand shroud (Fig. 9**b**). In the example of Figure 9**c**, both running out of reactive sites and steric hindrance affect the type and amount of adsorbed species after saturation has taken place.

To know whether running out of reactive sites or steric hindrance (or perhaps yet another factor) determines saturation is not trivial. Simple geometric calculations can be made to estimate whether steric hindrance is taking place. Physisorbed monolayer of the ligands (Fig. 7**b**), with the simplifying assumption that ligands are arranged as a two-dimensional close-packed layer, can serve as a reference for the theoretical maximum obtainable ligand packing per unit area (36,43). The chemisorbed monolayer should have less ligands per unit area than the theoretical close-packed maximum, as the ligands are at specific locations defined by chemical bonding and not free to move to the closest packing (Fig. 7**a**). As an example, considering the TMA-water process, an experimentally measured ligand packing of 5–6 methyl groups per square nanometer corresponds to 70–80% of the maximum packing with methyl groups with van der Waals radius of 0.20 nm, and steric hindrance analogous to Figure 9**c** has been concluded as the saturation-determining factor (44). When steric hindrance determines saturation, in a series where other factors remain constant while the ligand size in ML_n is increased stepwise, a larger ligand size should result in a lower GPC. Such trends have been observed, for example, for growth of titanium dioxide thin films from alkoxide reactants (45) and growth of nickel oxide from β-diketonate reactants (46).

3.6. Growth Modes. How the units of the ALD-grown material are arranged on the surface is described by the *growth mode* (10,37). The arrangement of material on the surface is determined both by kinetic and thermodynamic processes, but this distinction is not often made in the ALD literature (11). How the material is arranged is usually investigated with surface-sensitive or nanometer-resolution methods, for example, low-energy ion scattering and transmission electron microscopy.

Three growth modes typically considered in ALD are shown in Figure 10. In *two-dimensional growth* (*Frank–van der Merwe growth*), the material layers fill up

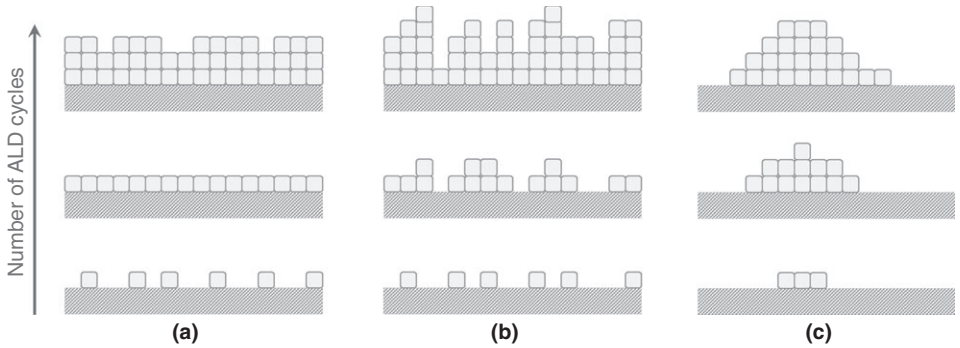

Fig. 10. Schematic illustration of various growth modes: (**a**) two-dimensional growth, (**b**) random deposition, and (**c**) island growth. Source: Puurunen (2020), Wikimedia Commons, Creative Commons Attribution 4.0 International license.

monolayer by monolayer. This is often the desired (even assumed) growth mode in ALD. In practice, perfect two-dimensional growth is rarely achieved (47). In *island growth* (*Volmer–Weber growth*), patches of ALD-grown material are observed instead of a continuous film, also when several bulk monolayer equivalents of the material have been grown by ALD. Initiation of growth from defect sites on an otherwise unreactive surface, such as hydrogen-terminated silicon, leads to island growth with a characteristic Type 2 substrate-inhibited growth trend with cycles (see Section 3.2) (33). Islands, or particles, also typically form in the ALD of noble-metal films on dielectric substrates, in a process that may involve surface diffusion (48). The choice of Reactant B may impact the island size and density (49). Island growth can sometimes be advantageous in ASALD (see Section 3.7). *Random deposition*, where the new material units have the same likelihood to attach on the underlying surface and the ALD-grown materials (50), is an intermediate reference case between two-dimensional growth and island growth. While the theoretical random deposition is unlikely to take place in practice, random deposition has value as a well-defined reference growth mode (51).

There appears to exist no straightforward relationship between the growth mode and crystallinity of the resulting ALD film. Island growth and (more) two-dimensional growth can both result in amorphous and crystalline films. Noble metal particles are an exception, as they are typically crystalline. The reactants, the resulting impurities, and the ALD temperature seem more important in determining crystallinity than growth mode (3).

3.7. Area-Selective ALD. ALD relies on site-specific chemisorption on surfaces. If there are no reactive sites, chemisorption cannot occur, and ALD growth does not take place. ASALD, where growth occurs selectively on one (or more) of the exposed surfaces, has become a growing field, for example, in semiconductor nanopatterning (52,53).

In ASALD, chemical dissimilarity is the driving force for differences between the *growth* and *nongrowth areas*. Growth occurs on the former but not on the latter surface, as illustrated in Figure 11. Typical dissimilar surfaces are hydrogen-terminated silicon, oxides such as SiO_2 and HfO_2, and metals such as Cu and Ru. In a favorable case, the ALD process grows 100% selectively on the

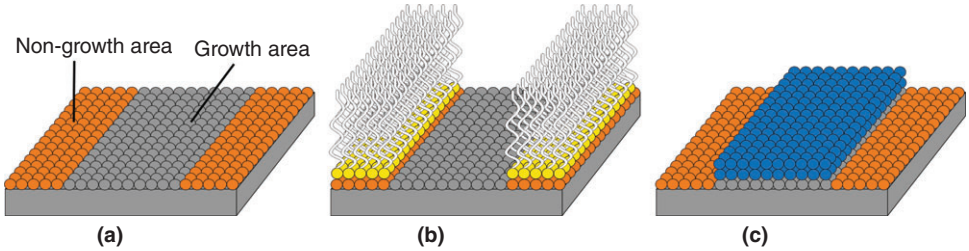

Fig. 11. Illustration of ASALD: (**a**) surface with chemically dissimilar areas, where ALD growth occurs (growth area) or does not readily occur (nongrowth area); (**b**) surface where a blocking agent has been selectively adsorbed on the nongrowth area; and (**c**) surface after completion of ASALD, where material has grown only on the targeted growth area. If the difference in selectivity between the two areas is large enough, a blocking agent is not needed, and step (**b**) can be skipped. Source: Based on Mackus et al. (52); van Ommen and Puurunen (2020), Wikimedia Commons, Creative Commons Attribution 4.0 International license.

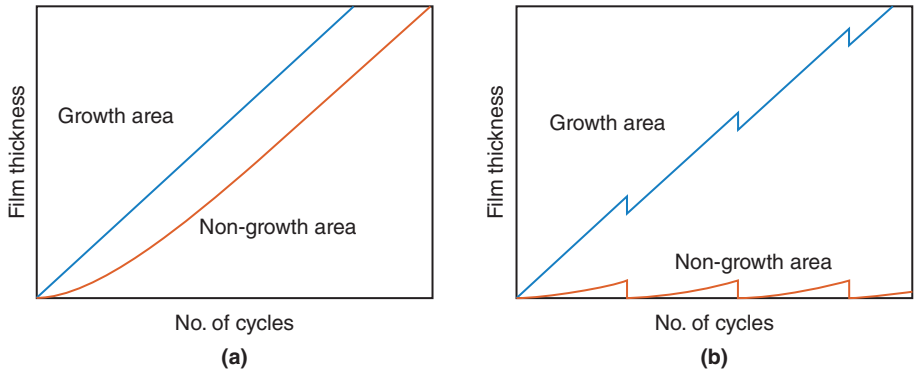

Fig. 12. Illustration of film thickness in growth and nongrowth areas (**a**) without intermittent etching steps and (**b**) with etching steps in between. Source: Puurunen and van Ommen (2020), Wikimedia Commons, Creative Commons Attribution 4.0 International license.

desired surface(s), leaving the other(s) intact. To create the nongrowth surface, blocking agents such as self-assembled monolayers preadsorbed on a specific surface may be used (Fig. 11**b**).

When thicker films are grown, island growth from defect sites often starts on the nongrowth surface as well, resulting in Type 2 substrate-inhibited growth (Fig. 12**a**). The selectivity S of area-selective deposition is often calculated by comparing the amount of material deposited onto the growth and nongrowth areas. In terms of thickness on the growth and nongrowth areas, t_{GA} and t_{NGA}, respectively (52,53), this gives $S = (t_{GA} - t_{NGA})/(t_{GA} + t_{NGA})$. One may exploit the high selectivity in the early cycles: etching and repassivation steps may be carried out to return the selectivity to the initial high level, as illustrated in Figure 12.

3.8. Growth Kinetics and Conformality. Detailed ALD surface chemistry is complex, with the various possible reaction mechanisms and saturation-determining factors. Kinetics of ALD are often modeled in a simplified way, assuming a lumped reaction that merges many reaction mechanisms into one or a few (54,55). The Langmuir adsorption formalism is almost always assumed to describe the ALD reaction steps (Step 1 or Step 3, Fig. 2), with the most simplest assumption of irreversible single-site adsorption (association): A (g) + * → A*. Here, A (g) denotes Reactant A in the gas phase, * denotes a surface site, and A* denotes A adsorbed on the surface site. In Langmuir adsorption, all surface sites are equal, and the adsorbed species are assumed not to interact with each other; a grid effectively visualizes the adsorption sites on the surface (Fig. 13). Release of gaseous by-products is typically not considered. The GPC is used to calculate the number of adsorption sites (in the simplified lumped reaction, one metal atom equals one adsorption site), and the surface coverage θ_A denotes the fraction of occupied sites. Kinetics are described through a reaction rate constant k or the (reactive) sticking coefficient c, where the sticking coefficient represents the fraction of impingements (from the kinetic theory of gases) with a vacant site that leads to attachment. An expression can be derived for the time-dependent surface coverage as function of the partial pressure as $\theta_A(t) = 1 - \exp(-k\, p_A\, t)$, where t is the reaction time. The main challenge is to access the reaction rate constant or sticking coefficient, as this is typically unknown.

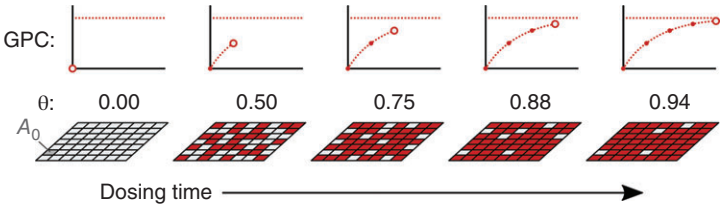

Fig. 13. Illustration of the Langmuir adsorption formalism for single-site irreversible adsorption. Source: Adapted from Arts et al. (56).

Conformality studies of ALD growth are a powerful tool to extract information on kinetic growth parameters, because the reaction kinetics determine how a 3D structure gets coated by a film. The ratio of intrinsic reaction rate to gas-phase diffusion rate, known, for example, in the field of heterogeneous catalysis as the *Thiele modulus (Th)*, has recently been introduced also in the field of ALD to characterize the evolution of conformality (54). If the reaction is fast compared to diffusion ($Th \gg 1$), the growth is *diffusion limited*, and the film growth saturates inside the structure much like a step function (Fig. 14**a**). If the reaction is slow compared to diffusion ($Th \ll 1$), the 3D structure gets filled with the reactant before reactions saturate, and the growth is said to be *reaction limited* (Fig. 14**b**). When coating large surface areas, the growth can also be *supply limited* (57). Sticking coefficient values can be extracted from experiments on well-defined 3D structures, where the characteristic *thickness profile* of the growth is exposed; lateral high-aspect-ratio (LHAR) structures, as illustrated in Figure 14, have emerged for this purpose (55,58). Different modeling approaches are used to simulate the thickness profiles, depending on the flow regime in the 3D structure. Many models operate in the *Knudsen flow* regime where the reactant merely collides with feature walls (mean free path ≫ limiting structure dimension, Knudsen number $Kn \gg 1$), while diffusion-reaction models are used for the *continuum flow* with frequent gas-phase collisions (54,55,59). Figure 15 shows example simulations for ALD thickness profiles: both exposure time t and the reactant partial pressure p strongly affect the penetration depth at half thickness ($PD_{50\%}$) (dose $= p \times t$; $PD_{50\%} \propto (p \times t)^{1/2}$), while the shape and slope of the thickness profile at the growth front depend on the sticking coefficient. Also, other parameters may play a role in determining the shape and position of the thickness profile. The field of thickness profile-based kinetic analysis is rather recent, and significant progress is expected in the future.

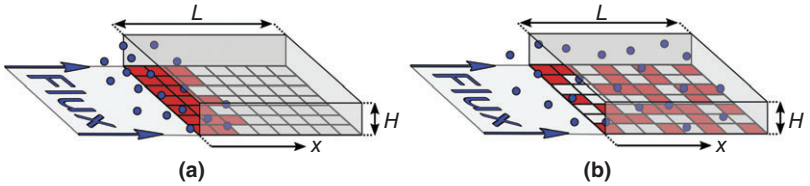

Fig. 14. Illustration of three-dimensional rectangular channels (LHAR structures) with (**a**) diffusion-limited growth (reaction rate is faster than diffusion rate, $Th \gg 1$) and (**b**) reaction-limited growth (diffusion rate is faster than reaction rate, $Th \ll 1$). Source: Courtesy of Arts co-workers (2020); adapted from the AtomicLimits Image Library.

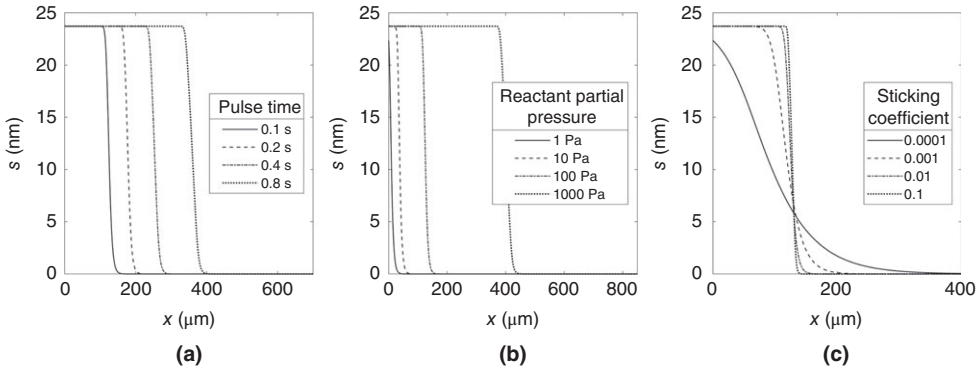

Fig. 15. Examples of ALD thickness profiles in rectangular channel LHAR structures simulated with a diffusion-reaction model (59) as a function of (**a**) Reactant A pulse time t, (**b**) Reactant A partial pressure p, and (**c**) sticking coefficient c. Parameters used in the simulation, if not otherwise stated: channel height H 500 nm, temperature 250°C, 250 cycles, inert carrier gas partial pressure 500 Pa, Reactant A molar mass 100 g/mol, inert carrier gas molar mass 28 g/mol, Reactant A diameter 0.600 nm, inert gas diameter 0.374 nm, adsorption capacity 4 metal atoms/nm^2, density of the material grown 3.5 g/cm^3, pulse time 0.1 s, Reactant A partial pressure 100 Pa, and sticking coefficient 0.01. Source: Verkama and co-workers (2020), http://doi.org/10.5281/zenodo.4354346. Creative Commons Attribution 4.0 International license.

3.9. Deviations From Ideality. The concept of ideal ALD, based on saturating and irreversible reactions, is a useful framework to understand and model ALD processes. However, most—if not all—ALD processes deviate from this ideal concept to some extent. Furthermore, suboptimal reactor design and poor selection of operating parameters may lead to conditions where nonidealities dominate. Figure 3 already showed some possible deviations from saturating, irreversible reactions characteristic for ideal ALD. This section explores in further detail typical deviations from ideality in real ALD processes. For a real ALD process, it depends on the A–B reactant pair, process temperature, and on other processing parameters (flows, pressures, etc.) how closely ideality can be approached. Recommended publications on nonidealities are the reviews (35) and (60).

Deviations from ALD conditions, as temperature is increased or decreased, are often discussed in terms of the ALD temperature window concept, or ALD window, in short. The ALD window concept was originally created by Suntola to illustrate how ALD conditions can, and cannot, be attained by changing the temperature. Figure 16 shows an adapted version of the ALD window concept.

Most reviews on ALD present the ALD window concept in some way. Unfortunately, often a flat, constant GPC with increasing temperature is assumed for growth within the ALD window. The authors of this article believe that an assumption of constant GPC with temperature within the ALD window is a misconception without a real scientific basis. Consequently, the GPC within the ALD window is here shown as a gray box (Fig. 16), where the GPC may vary in many ways (see Fig. 6). Within the ALD window, the GPC varies because of changes in the reaction mechanisms with temperature, in numbers and types of adsorption sites, and in crystallinity. Inside the ALD window, the trends in the amount grown with temperature are typically significantly weaker than outside

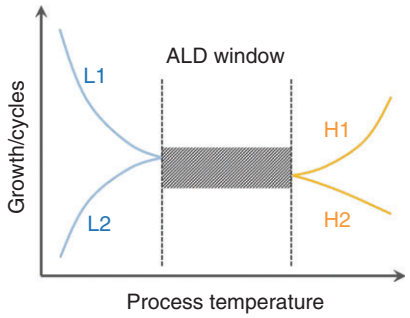

Fig. 16. Illustration of the ALD temperature window concept. Inside the ALD window (gray area), the process fulfills the criteria of ALD. Outside the ALD window, the process fails to fulfill the ALD criteria, because of (L1) reversible multilayer adsorption (physisorption); (L2) activated chemisorption, not saturated; (H1) thermal decomposition of the reactant; or (H2) desorption due to reversible reactions. Source: Adapted from Suntola (20). Puurunen and van Ommen (2020), Wikimedia Commons, Creative Commons Attribution 4.0 International license.

of the ALD window. The following paragraphs deal with the four mechanisms of deviation from ideal ALD of the classical ALD window plot and additional nonidealities.

Thermal reactant decomposition (H1). Perhaps the most typical deviation from the ALD characteristics for a reaction is a nonsaturating component through reactant decomposition on the surface (Fig. 3**c**). Such undesired decomposition typically becomes more prominent with higher process temperature and longer reaction times. The latter becomes especially important when dealing with large batches and high-surface-area substrates. Some reactants start to decompose already at temperatures below 150°C, while others may be safely used without decomposition up to well over 500°C. This type of decomposition can be found, for example, for the TDMAT reactant on TiN surface (61). Nonsaturation through reactant decomposition on the surface is shown in Figure 3**b**,**c** and is labeled as H1 in the ALD window image (Fig. 16).

Sometimes, reactant decomposition is catalyzed by a surface. The reaction of a gaseous compound can be saturating and irreversible at a given temperature on one surface, but on another surface (either another substrate or the ALD-grown material itself), the saturating characteristic may be lost. An example of such surface-catalyzed reactant decomposition is the decomposition of metalorganic Cu reactants by a CuO_x surface (62). Somewhat similar phenomena take place in PEALD, where the recombination probability of radicals strongly depends on the nature of the surface (30,56).

Temperature-induced desorption (H2). Chemical processes are in principle reversible. Chemisorption is irreversible in the timescale of the ALD process, if the activation energy of desorption (reverse reaction of chemisorption) is sufficiently large for desorption not to occur. Equilibrium reactions can also be driven toward the products by removing the reaction products; this is often practiced in ALD using a continuous flow of carrier gas. When temperature is increased, material eventually may desorb, either simply reversing the adsorption process that took place or as some chemically altered species. Reversible chemisorption is

shown in Figure 3**e**, and desorption is labeled as H2 in the classical ALD window image (Fig. 16).

Multilayer physisorption (L1). In physisorption, adsorption takes place through reversible processes that resemble condensation from vapor to liquid phase. Physisorption processes are neither site specific nor limited to one layer only: depending on the temperature and partial pressure conditions, multilayers may form (Fig. 7). Physisorption is reversible and sensitive to the partial pressure of the reactant: when purging starts, desorption starts. Physisorption does not result in the self-terminating reactions required in ALD. Physisorption is shown in Figure 3**f** and labeled as L1 in the classical ALD window image (Fig. 16).

Slow reactions with insufficient reaction time/dose (L2). Chemisorption can saturate slowly. At conditions that, in principle, enable saturation, saturation may not be reached if given insufficient time or dose. Kinetics depend on temperature: the lower the temperature, the more time it takes for reactions to saturate, especially if an activation barrier has to be overcome for chemisorption to occur. Nonsaturation due to insufficient time/dose is shown in Figure 3**g** and labeled as L2 in the classical ALD window image (Fig. 16).

Overlapping reactant pulses. ALD relies on separated reactions (Steps 2 and 4 in Fig. 2). The reactions are separated typically by purging with inert gas or by evacuation or sometimes a combination of the two. The reactant pulses can overlap because of too short purge or evacuation times or by leaks into the system—either an actual leak or a virtual leak, for example, from cold spots in the reactor. If Reactants A and B are simultaneously present in the gas phase, they can react with the surface or in the gas phase, leading to non-self-limiting CVD. Typically, this CVD component decreases the layer uniformity, as it manifests itself more on certain parts of the ALD reactor, for example, the place where mixing of the reactant feeds takes place. Optimizing the purge times is typically part of the optimization of an ALD process in terms of product quality versus productivity (throughput); lower process temperatures typically require longer purge times (32).

Competitive adsorption of gaseous by-products. Sometimes, gaseous reaction by-products formed in an ALD process are not inert, as preferred, but *reactive*. If the by-products react with the same surface sites as the ALD reactants, they can block the sites from reacting with the ALD reactants and cause gradients in the film. A classic example of reactive gaseous by-products causing gradients in films is hydrogen chloride, formed in the reaction of metal chlorides with hydroxyl groups. An example of a thickness profile measured for the $TiCl_4$–H_2O reaction can be found in Reference (59): there is no constant plateau as ideally expected but a slow decrease, likely because of the readsorption of HCl.

Etching. Some gaseous molecules used as in ALD may also etch away species from the surface, instead of adsorbing onto it. This etching may be limited to a single layer or proceed to deeper layers. A classic example where etching takes place at higher temperatures is the reaction of $TaCl_5$ with oxide surfaces, where surface oxygen is etched and gaseous $TaOCl_3$ formed (63). Reactions where gaseous species exchange parts with a surface, without adsorbing, have been called *nongrowth ligand-exchange reactions* (64). In growth of nanolaminated materials or alloys, the process used to grow one material can etch away the other composite materials, leading to enrichment of the first material in the

film being grown. The combination of the diethyl zinc–water and TMA–water processes, to make ZnO/Al_2O_3 nanolaminates and alloys, is a typical example where etching occurs, as Zn may be etched by TMA, giving Zn deficiency in the films (65). Surface etching that limits itself to a single layer is exploited in *atomic layer etching*, a fast-developing technology closely related to ALD (66,67).

Subsurface processes. In some cases, the modification of a material in gas–solid reactions is not limited to adsorption on the surface but proceeds to subsurface regions, through various mechanisms.

In addition to adsorption, *absorption* may take place in the growing film. (The term *sorption* can be used to cover both adsorption and absorption.) A characteristic example of absorption is the formation of subsurface oxygen in the growing ALD material during combustion-based noble-metal processes, for example, ruthenium (68). The absorption process is not limited to a chemisorbed monolayer, so the characteristic saturation-control feature of ALD ceases to exist. For example, in the case of ruthenium, sorption of an equivalent of three monolayers of oxygen has been concluded (68). When subsurface absorption takes place, the details of sorption and amounts sorbed depend on the temperature, partial pressure, and time.

ALD process may possess an oxidizing or reducing character that modifies the underlying substrate. Combustion-based noble-metal processes using oxygen or ozone as Reactant B typically oxidize the substrate and therefore are incompatible with oxidation-sensitive substrate materials. Also, other types of Reactants B may oxidize the substrate: water as Reactant B leads to the growth of silicon oxide on originally oxide-free silicon during the ALD of oxides (69). An example of reduction is the ALD of TiO_2 from tetrakis(dimethylamino)titanium(IV) and water, which causes the reduction of underlying γ-Fe_2O_3 to Fe_3O_4 (magnetite) (70). The substrate modification can be desired, as in the case of the formation of Fe_3O_4/TiO_2 core/shell nanoparticles (70), or undesired, as in the case of the oxidation of silicon (69).

Vapor-phase infiltration can be seen as a distinct method evolved from ALD, where subsurface processes are deliberately exploited. In vapor-phase infiltration, an inorganic material is grown by ALD inside a polymeric or other soft material. The ALD reactant diffuses inside the polymer and reacts either with functional sites of the polymer in the subsurface area or with the second reactant before outdiffusion has taken place (8,71).

Another method sharing the self-limiting feature with ALD is the rapid vapor deposition (RVD) of silica nanolaminates (72). In RVD, a metal (eg, aluminum) catalyzes the polymerization of tris(*tert*-butoxy)silanol in a process that self-limits because of diffusion limitations. The thickness per cycle goes through a maximum with temperature, being about 12 nm (more than 32 SiO_2 monolayers). Self-terminating chemisorption does not take place, but multilayer growth occurs, differentiating RVD from ALD.

Partial pressure effects. Ideally, the characteristics of a surface after completed ALD reactions should not depend on the partial pressure of the reactants: in saturating, irreversible adsorption, the end result at saturation is the same for different partial pressures. Nevertheless, partial pressure effects have been observed in some cases. Subsurface processes, partial reversibility of reactions, and surface diffusion may be responsible for such effects.

In some cases, the partial pressure of a reactant may determine the chemical nature of the material being grown. Especially in the case of combustion-based noble metal ALD processes, the partial pressure of the oxidizing reactant, for example, oxygen, may determine whether a metallic or oxide film is formed. Such effect has been observed, for example, for Ru and RuO_2 (73). Interestingly, in a study employing 3D LHAR structures and an ozone-based iridium process, at the entrance of the structure an iridium oxide thin film was detected, while deeper inside the LHAR structure, the film was metallic (74). In LHAR structures, the partial pressure of the reactant decreases when going inside the structure (59), so the observation of iridium oxide at the entrance may be linked to a higher partial pressure of ozone.

There is evidence that the partial pressure of the reactant may sometimes influence the GPC. If in the noble-metal ALD processes, a chemisorbed monolayer does not form and the amount of subsurface oxygen is not saturating to a certain level, then a dependency of the GPC on the oxygen dose is expected. Also, studies exist where a low/high water dose has been concluded to affect the GPC in metal oxide ALD processes (75). It seems likely that the water reaction in the growth of Al_2O_3 has a minor reversible, partial-pressure-dependent component (58).

Recently, an effect of the oxygen partial pressure on platinum nanoparticle growth and particle size distribution (PSD) has been demonstrated (76). Depending on the partial pressure of oxygen (Reactant B), the reaction rate strongly varies, to the extent that low partial pressures can effectively suppress growth within the timeframes typically used in ALD. For low partial pressures, single atoms were left on the surface, whereas for higher partial pressures, nanoparticles of even 6 nm were formed after only five cycles. The mean particle size and the shape of the PSD further depended on the partial pressure. Here, partial-pressure-dependent surface diffusion and particle coalescence seem to play a role.

4. Reactants and Processes

4.1. General Overview. In a typical ALD process, two reactants (Reactants A and B) are used sequentially for the growth of a solid inorganic material. These reactants are usually identified as *metal* and *nonmetal reactants*, respectively. Depending mainly on the selection of the nonmetal reactant of the two-reactant ALD process, different classes of materials such as metal oxides, nitrides, chalcogenides, phosphides, arsenides, and halides along with pure and alloy elemental (metal) materials can be grown, as shown in Figure 17.

The shift of interest toward multicomponent materials, coupled with the precise control over the composition of the grown material that ALD schemes enable, resulted in adopting, also, more complex reaction sequences. These, often coined as *multistep* type $[(ABC)_x$ or $(ABCD)_x]$ or even *supercycle* type $[[(A_1B_1)_m(A_2B_2)_n]_x]$ reaction sequences (77) have enabled the deposition of laminates and other complex materials.

4.2. Desired Characteristics of ALD Reactants. The most important properties for an ALD reactant are (*1*) sufficiently high *volatility* at temperatures lower than the ALD reaction temperature, (*2*) *thermal stability*, with

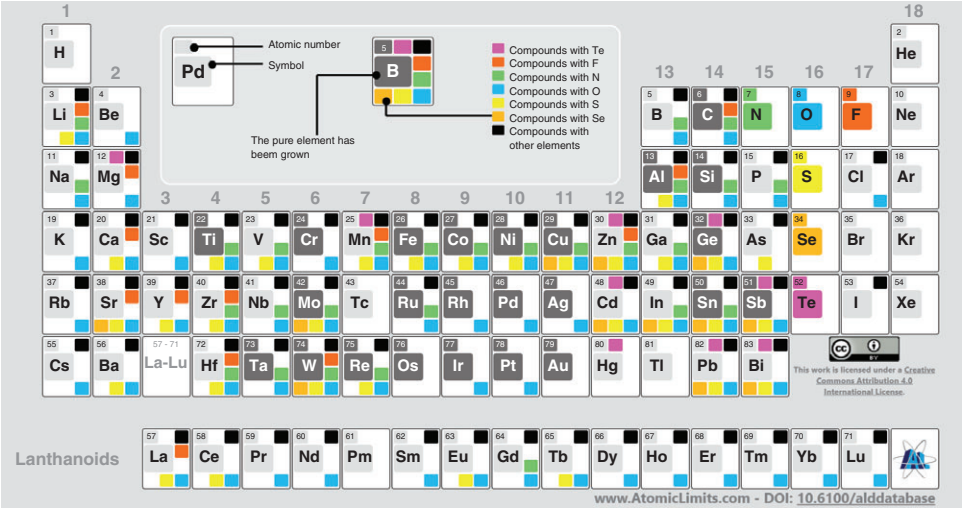

Fig. 17. Periodic table overviewing the types of materials grown by ALD, from https://doi.org/10.6100/alddatabase (as of 21 December 2020), updating info from Miikkulainen and co-workers (3). Growth of pure elements (dark-gray shading around white symbol) is reported together with the growth of different other classes of materials: chalcogenides, namely, sulfides (yellow), selenides (light orange), and tellurides (violet); halides, namely, fluorides (orange), nitrides (green), and oxides (blue); and compounds with other elements (black). Source: ALD Periodic table. Retrieved from: https://doi.org/10.6100/alddatabase. Creative Commons Attribution 4.0 International License.

no thermal self-decomposition nor etching of or adsorption in the growing material, and (*3*) saturating and irreversible *reactivity* (fast and aggressive self-terminating reactions with nonreactive/inert and volatile by-products) that results in surface active sites repopulation. Thermogravimetry-differential thermal analysis (TG-DTA) (analysis of the compound's mass loss rate as a function of temperature) is often used to assess the first two parameters of an ALD (metal) reactant (Fig. 18). In addition, in order to be practically applicable, ALD reactants should preferably (*1*) be safe and easy to synthesize and handle, (*2*) cause, either directly or via their reaction by-products, minimal corrosion on the process equipment used, (*3*) result in minimal impurities on the grown materials, (*4*) show considerable shelf-life, also under elevated temperature often used for their vaporization, (*5*) be inexpensive, and (*6*) be nontoxic. As a rule of thumb, (metal) reactants used for CVD can be considered as candidate reactants for ALD, given the prerequisite that they do not self-decompose in the gas phase.

4.3. Categories of ALD Reactants. ALD reactants are typically categorized into two main classes: metal and nonmetal reactants, as summarized in Tables 1 and 2, respectively (3,10,77). Metal reactants (also sometimes called precursors or reagents) can be further split into two distinct classes of materials: inorganic and metalorganic. If a direct metal–carbon bond is included in the reactant molecule, then the metalorganic material can be further subclassified as organometallic. Metal elements and halides are considered typical representatives of inorganic metal reactants, while metal alkoxides, β-diketonates, amides (and their alkylated and silylated derivatives), imides, amidinates

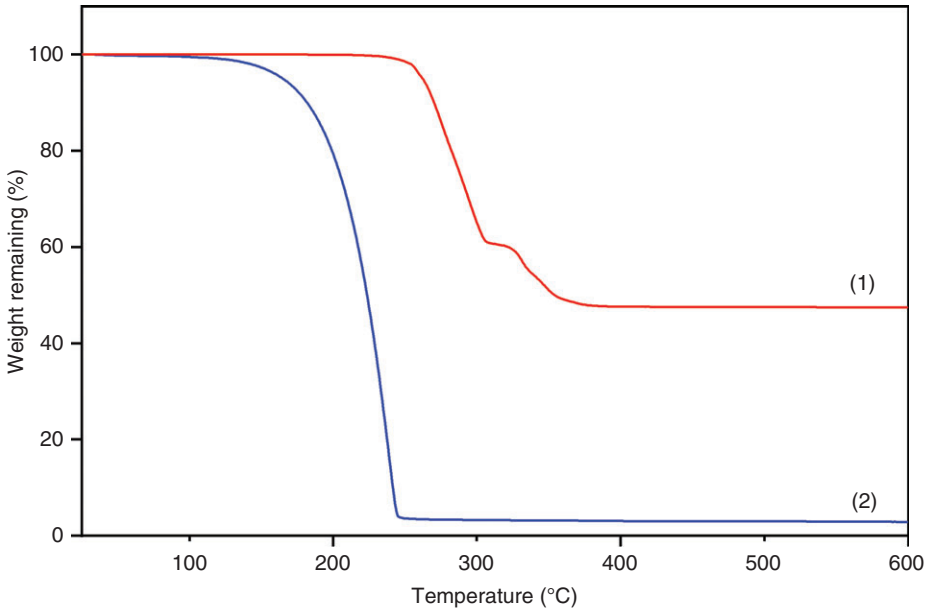

Fig. 18. Thermogravimetric analysis of two ALD metal reactants with different volatilization behavior as examples. The first case (a Bi acetate, $Bi(O_2CMe)_3$) shows weight loss due to thermal decomposition accompanied by only some volatility at elevated temperatures, leading to a large residual mass. Contrarily, the second case (a Bi alkoxide, $Bi(OCMe_2{}^iPr)_3$) shows volatility from a much lower temperature onset with negligible residual mass, indicating no thermal self-decomposition. Source: Data from (78). Courtesy of Timo Hatanpää 2020.

(and acetamidinates), phosphines, alkyls, cyclopentadienyls, and carbonyls are considered typical reactants of the metal organic class.

For the metal reactants, the incorporation of ligand(s) around the metal center is beneficial for enabling the delivery in the gas phase and ensuring the self-terminating nature of the process. The choice of the (metal) reactant ligand types is nontrivial and often results from an optimization of molecular parameters (volatility, stability, reactivity, and ligand size) together with process- and growth-related parameters. Recently, combinations of ligand functionalities have also been explored by heteroleptic chemistry in an effort to tune by design the properties of ALD reactants (79).

For the nonmetal reactants, hydrides of elements are mostly considered, with typical sources including simple molecules such as water, ammonia, hydrogen sulfide, and hydrogen fluoride. Also, more reactive radical sources, such as ozone, and energy-activated species, such as oxygen and hydrogen plasma, can be used. Alkyl and silyl compounds have also been reported for the growth of metal carbides and metals, respectively. Alcohols have been reported for the growth of mostly metal oxides. In certain processes, a catalyst (typically an amine) is used (80,81). Sometimes, one compound can be used as both a metal and a nonmetal reactant for the deposition of metal and oxygen, respectively, such as metal alkoxides reacting with a metal chloride (69,82).

Table 1. **Classification of Metal Reactants Typically Used on ALD Processes (3,10,77)**

Class *(*Subclass)*	Type	Ligands[a]	Ligand example
inorganic	elements	no ligand	no ligand
	halides	F, Cl, Br, I	chloride (Cl)
metal organic	alkoxides	OMe, OEt, O^{n}Pr, O^{i}Pr, O^{n}Bu, O^{i}Bu, O^{t}Bu, O^{t}Pe, mmp, dmb, mp	methoxy (OMe)
	β-diketonates	acac, tmhd, thd, tod, od, edmdd, methd, hfac, OAc, O_2C^tBu	acetylacetonato (acac)
	amides	NH_2, NMe_2, NEtMe, NEt_2, NH^{t}Bu	amido (NH_2)
	imides	NEt, N^{i}Pr, N^{t}Bu, N^{t}Am	ethylimido (NEt)
	amidinates	MeAMD, ^{i}PrAMD, ^{i}PrfAMD, ^{t}BuAMD, ^{s}BuAMD, ^{i}PrGuan, $(^iPrN)_2CNMe_2$	*N,N′*-dimethylamidinato (MeAMD)
	phosphines	PEt_3, P^{n}Bu$_3$	triethylphosphine (PEt_3)
**Organometallic*	alkyls	Me, Et, ^{i}Pr, All, ^{n}Bu, ^{i}Bu, ^{t}Bu, Np	methyl (Me)
	cyclopentadienyls	Cp, CpMe, $CpMe_5$, CpEt, Cp^{i}Pr, Cp^{i}Pr$_3$, Cp^{t}Bu$_3$, Cp^{n}PrMe$_4$	methylcyclopentadienyl (Cp)
	carbonyls	CO	carbonyl (CO)

[a]Ligand abbreviations corresponding to alkoxide ligands: methoxy [OMe], ethoxy [OEt], *n*-propoxy [O^{n}Pr], isopropoxy [O^{i}Pr], *n*-butoxy [O^{n}Bu], isobutoxy [O^{i}Bu], *tert*-butoxy [O^{t}Bu], *tert*-pentoxy [O^{t}Pe], 1-methoxy-2-methyl-2-propoxy [mmp], 2,3-dimethyl-2-butoxy [dmb], 3-methyl-3-pentoxy [mp]; β-diketonate ligands: acetylacetonato [acac], 2,2,6-trimethyl-3,5-heptanedionato [tmhd], 2,2,6,6,-tetramethyl-3,5-heptanedionato [thd], 2,2,6,6-tetramethyl-3,5-octanedionato [tod], octane-2,4-dionato [od], 6-ethyl-2,2-dimethyl-3,5-decanedionato [edmdd], 1-(2-methoxyethoxy)-2,2,6,6-tetramethyl-3,5-heptanedionato [methd], 1,1,1,5,5,5-hexafluoroacetylacetonato [hfac], acetato [OAc], 2,2-dimethylpropionato [O_2C^tBu]; amide ligands: amido [NH_2], dimethylamido [NMe_2], ethylmethylamido [NEtMe], diethylamido [NEt_2], *tert*-butylamido [NH^{t}Bu]; imide ligands: ethylimido [NEt], isopropylimido [N^{i}Pr], *tert*-butylimido [N^{t}Bu], *tert*-amylimido [N^{t}Am]; amidinate ligands: *N,N′*-dimethylamidinato [MeAMD], *N,N′*-diisopropylacetamidinato [^{i}PrAMD], *N,N′*-diisopropylformamidinato [^{i}PrfAMD], *N,N′*-di-*tert*-butylacetamidinato [^{t}BuAMD], *N,N′*-di-*sec*-butylacetamidinato [^{s}BuAMD], *N,N′*-diisopropylguanidinato [^{i}PrGuan], *N,N′*-diisopropyl-2-dimethylamidoguanidato [$(^iPrN)_2CNMe_2$]; phosphine ligands: triethylphosphine [PEt_3], tributylphosphine [P^{n}Bu$_3$]; alkyl ligands: methyl [Me], ethyl [Et], isopropyl [^{i}Pr], allyl [All], *n*-butyl [^{n}Bu], isobutyl [^{i}Bu], *tert*-butyl [^{t}Bu], neopentyl [Np]; cyclopentadienyl ligands: cyclopentadienyl [Cp], methylcyclopentadienyl [CpMe], pentamethylcyclopentadienyl [$CpMe_5$], ethylcyclopentadienyl [CpEt], isopropylcyclopentadienyl [Cp^{i}Pr], tri-isopropylcyclopentadienyl [Cp^{i}Pr$_3$], tris(*tert*-butyl)cyclopentadienyl [Cp^{t}Bu$_3$], *n*-propyltetramethylcyclopentadienyl [Cp^{n}PrMe$_4$]; carbonyl ligands: carbonyl [CO].

4.4. Typical Processes Examples. In this section, three examples, each representative for a larger class of important ALD processes, are provided. Simplified reaction schemes of these processes are shown in Figure 19.

The TMA–water (Me_3Al/H_2O) process to grow Al_2O_3 is often regarded as an archetypical example of ALD processes (5,10,11). This process illustrates the principles of ALD well as (*1*) it represents a thermal ALD process with a highly reactive metal reactant that fulfills well the requirement of reaction

Table 2. **Classification of Nonmetal Reactants Typically Used on ALD Processes (3,10,77)**

Type		Compounds[a]	Mostly used to deposit
hydrides	*(pnictogen)*	NH_3, NH_3 plasma, N_2H_4	metal nitrides
		PH_3	metal phosphides
		AsH_3	metal arsenides
	(chalcogen)	H_2O, H_2O_2	metal oxides
		H_2S	metal sulfides
		H_2Se	metal selenides
		H_2Te	metal tellurides
	(halogen)	HF	metal fluorides
elements (molecular)		H_2, H plasma	metals
		O_2, O_3, O plasma	metal oxides
		N plasma	metal nitrides
alcohols		*R*OH	metal oxides
other	*(alkyls)*	BEt_3	metal carbides
	(silanes)	Si_2H_6	metals

[a]Typically used nonmetal reactants reported based on type: ammonia [NH_3], hydrazine [N_2H_4], phosphine [PH_3], arsine [AsH_3], water [H_2O], hydrogen peroxide [H_2O_2], hydrogen sulfide [H_2S], hydrogen selenide [H_2Se], hydrogen telluride [H_2Te], hydrogen fluoride [HF] (hydrides); hydrogen [H_2], oxygen [O_2], ozone [O_3] (elements); alcohols [*R*OH, *R* denotes organic chains] (alcohols); triethylborane [BEt_3], disilane [Si_2H_6] (other).

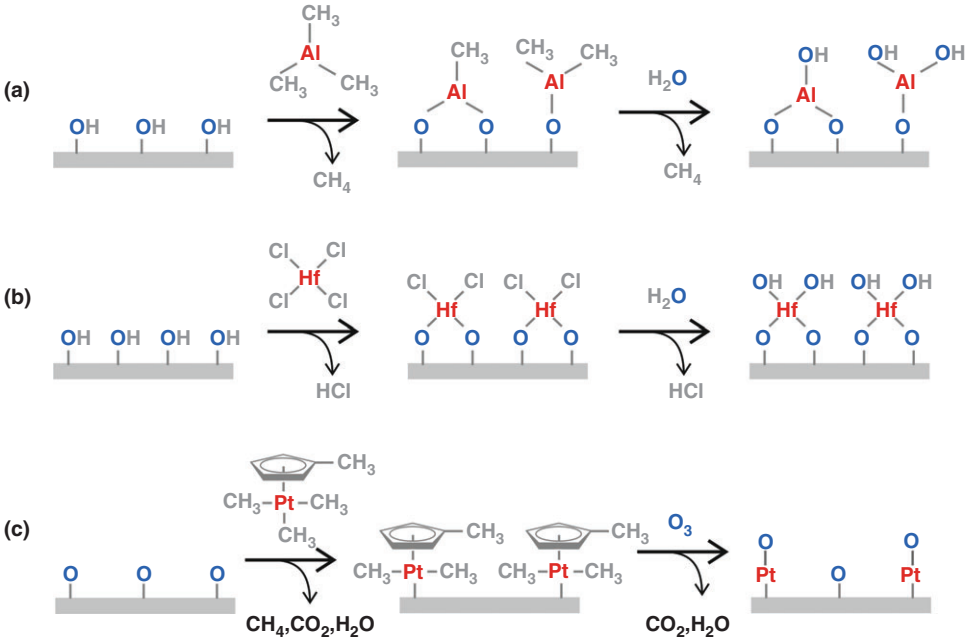

Fig. 19. Simplified reaction scheme illustration for three typical ALD processes: (**a**) Me_3Al/H_2O to grow Al_2O_3, (**b**) $HfCl_4/H_2O$ to grow HfO_2, and (**c**) $MeCpPtMe_3/O_3$ to grow Pt. Source: van Ommen and Puurunen (2020), Wikimedia Commons, Creative Commons Attribution 4.0 International license.

self-termination also in complex topologies; (*2*) it involves the deposition of the most frequently grown class of ALD materials, oxides, with the most commonly used type of nonmetal reactant, nonmetal hydride; (*3*) the reaction by-product, methane, is inert; and (*4*) it is a process with large industrial significance (12) and thus is one of the most widely studied ALD processes (3). Both Me_3Al and H_2O are highly reactive and thermally stable under the typically selected ALD reaction temperature range of 200–300°C, resulting in GPC on the order of 0.1 nm or about one-third of an average monolayer of Al_2O_3 (5,10) ($\overline{h}^{ml} = 0.30$ nm, assuming $\rho = 3.2$ g/cm^3). Ligand-exchange reaction, releasing methane, is the primary reaction mechanism (10). It has been suggested that a combination of steric hindrance by methyl groups determines saturation after reactive ||–OH groups have been consumed (10). The reactions are highly exothermic, with reaction enthalpies of −343 and −251 kJ/mol for the Me_3Al (Step 1) and H_2O (Step 3) reactions, respectively (83). The overall reaction is as follows, and a simplified reaction scheme is shown in Figure 19**a**.

$$Al(CH_3)_3(g) + \frac{3}{2}H_2O(g) \rightarrow \frac{1}{2}Al_2O_3(s) + 3CH_4(g) \quad (1)$$

The hafnium chloride–water ($HfCl_4/H_2O$) process to grow HfO_2 is another characteristic example of an ALD process. This process results in a GPC of about 0.04 nm (84) (ca 10% of an average monolayer of HfO_2; $\overline{h}^{ml} = 0.33$ nm, assuming $\rho = 9.7$ g/cm^3). Ligand-exchange reactions release hydrogen chloride as gaseous by-product, which potentially may interact with the surface. For surfaces with a low number of ||–OH groups, it has been suggested that the number of available reactive groups determines saturation (84). The overall reaction is as follows, and a simplified reaction scheme is shown in Figure 19**b**.

$$HfCl_4(g) + 2H_2O(g) \rightarrow HfO_2(s) + 4HCl(g) \quad (2)$$

Noble metals can be grown by ALD using processes where a metal reactant is combined with an oxidizing agent, such as oxygen and ozone. A well-known example is the $MeCpPtMe_3/O_3$ process to grow platinum (48,85,86). This process is based on combustion of the ligands by gaseous (during Step 3) and sorbed (during Step 1) oxygen, yielding a GPC of about 0.05 nm in the regime of constant growth (85) (ca 20% of an average monolayer of Pt; $\overline{h}^{ml} = 0.25$ nm, assuming $\rho = 21.5$ g/cm^3). Noble metal ALD processes frequently have a nucleation delay, as in substrate-inhibited ALD (see Section 3.2). The simplified overall reaction based on complete combustion is as follows, and a simplified reaction scheme is shown in Figure 19**c**.

$$(CH_3C_5H_4)Pt(CH_3)_3(g) + 8O_3(g) \rightarrow Pt(s) + 9CO_2(g) + 8H_2O(g) \quad (3)$$

5. Reactors, Substrates, and Process Conditions

Equipment for carrying out ALD is often designed considering the reaction processing requirements—especially temperature—along with the type of substrates coated and the delivery requirements of the reactants. In the microelectronics

industry, the most widely adopted environment of ALD systems, it is common practice to operate the equipment in a process-specific, dedicated way inside a cleanroom environment. Although often classified based on the type of the reactor chamber—the system's core—these systems typically comprise a number of different modules required to store and deliver the reactants, purge and treat the reaction by-products, provide heating for different parts including preheating of the substrates, and load/unload the substrates.

A wide range of substrate materials have been processed with ALD (11). Most of them are inorganic materials that rely on some initial surface functionality for ALD growth to occur (often hydroxyl-terminated surfaces, eg, oxides); however, metals and surfaces considered relatively inert (eg, graphene) have also been coated. ALD coatings have also been grown on organic materials (polymers and paper fibers) whose subsurface can be modified in a top-down approach by vapor-phase infiltration (8), (71). In terms of shape, there is little limitation for ALD, with materials varying from highly porous particles (87) and porous membranes (88) to wafers with high-aspect-ratio structures (55) and flexible foils (89) having been coated by ALD.

Different classifications of ALD reactor systems can be made depending on the processing and productivity viewpoints of their use (90); see Figure 20. The injection and distribution together with the flow direction of the reactants over the coated substrates and the configuration of the energy source used for the activation of the reactive species are typically listed as processing parameters. The type, amount, and configuration of substrates handled—and to a lesser extent the pressure-operating regime—together with the ALD mode of operation are often used as productivity descriptors for the systems. A summary of this classification is given (Fig. 20 and Table 3).

ALD reactants can be gaseous, liquid, or solid at room temperature. The delivery of gases is relatively simple: a pressure-regulated bottle typically suffices for their direct feed. For the liquids, often overflow bottles or bubblers and the use of a carrier gas (typically inert gases: Ar, N_2, or He) are implemented; precise temperature control is important for uniform delivery. For high productivity, when the needs for reactant delivery are high, direct liquid injection (DLI) can offer a solution for achieving stable vapor flow. Delivery of solid ALD reactants is more challenging, often requiring complex structured source containers (sublimators) that ensure carefully controlled temperature uniformity and gas/solid mixing during delivery. Given the self-terminating character of the ALD processes and the economics of reactants utilization, it is essential to ensure consistent dosing of the ALD reactants. An estimation can be made based on the duration/time of exposure (feeding time) multiplied by the reactant concentration expressed as a function of canister temperature and pressure. In practice, the timings selected are often in the regime of some overexposure, and a considerable part of the precursor may not be used (91). Process lines need to be adequately heated, adopting an increasing temperature gradient toward the reactor chamber, in order to prevent condensation of vaporized liquid and solid reactants onto cold spots. In addition, pulsing valves used for the separation of the reactants need to be fast (to accommodate for short cycling times) and of high duty (to endure the large number of actuation required over a system's lifetime), with small dead volumes and often integrated heating.

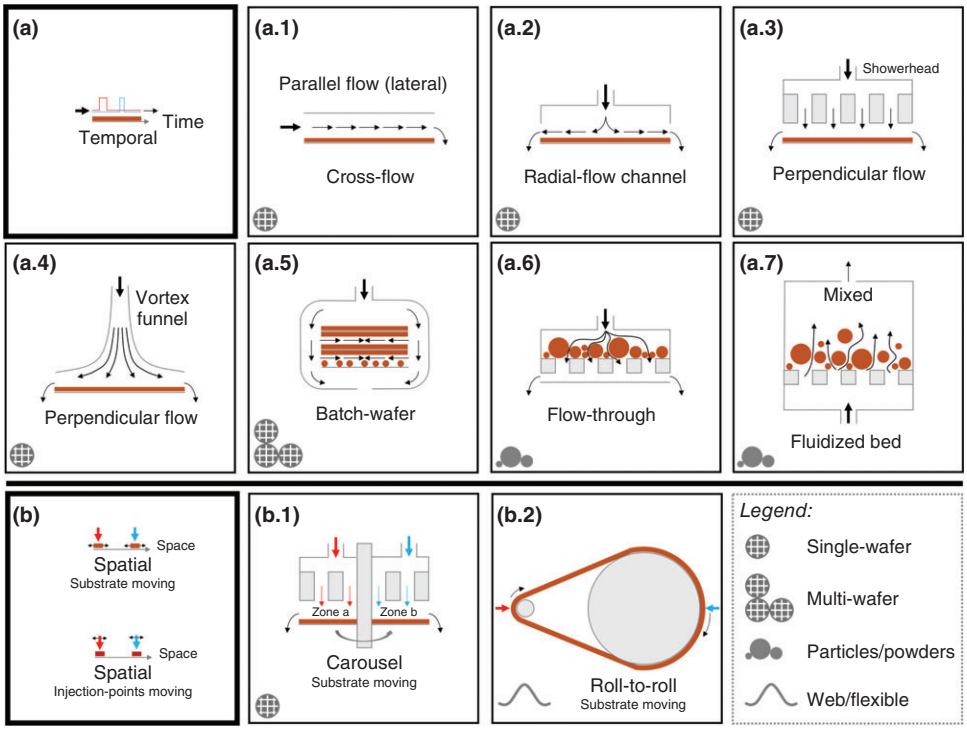

Fig. 20. Classification of temporal (**a**, top) and spatial (**b**, bottom) ALD reactor systems based on distribution and flow direction of the reactants. Flow-type reactors for temporal ALD include the cross-flow reactors (flow channel or traveling wave, **a.1**), radial-flow channel reactors (**a.2**), and perpendicular-flow reactors based on top injection (utilizing a showerhead in (**a.3**) or a vortex funnel in (**a.4**) for distribution of the gaseous reactants). Several process variants for productivity increase (batch-wafer reactor in (**a.5**), based on cross-flow reactor) and for particles/powders processing (flow-through reactor in (**a.6**) and fluidized bed reactor in (**a.7**) reactors) are shown. A carousel reactor (**b.1**) and a roll-to-roll reactor (**b.2**) for spatial ALD are also illustrated. Source: Goulas and co-workers (2020), Wikimedia Commons, Creative Commons Attribution 4.0 International license.

Table 3. **Classification of ALD Equipment Based on Processing Parameters**

Basis of classification	Options
substrate type	wafer, web or other flexible, particles/powders, objects
substrate configuration	single-wafer, multi-wafer, batch-wafer, carousel, roll-to-roll
ALD mode	temporal, spatial
reactants injection and distribution	cross-flow, single-hole top injection, multiple-hole top injection (showerhead), single-hole top injection (vortex funnel) (convective); varied between boat (convective) and wafers (diffusive)
flow direction over the substrate	parallel flow (lateral), perpendicular flow (stagnant), radial-flow channel, flow-through, mixed
energy activation	thermal (hot wall, cold/warm wall), radical enhanced, plasma enhanced (direct, remote, or combination), photo-assisted, hot-wire assisted

The purpose of the reactor chamber is to provide the necessary environment for allowing the reactant gases to efficiently reach and react with the substrates under process conditions that ensure ALD. To achieve a sufficient reactivity of Reactants A and B, the reactor chamber is heated directly (hot wall) or indirectly (cold/warm wall) to temperatures that can typically range up to 400°C (92). ALD reactors can have different configurations (77) for reactant injection and distribution where in most cases (cross-flow, single-hole top injection, and multiple-hole top injection/showerhead) gas transport is realized on a convective flow regime (as shown in Fig. 20). Vertical multi-wafer batch reactors operate with a convective flow on the boat level (the structure containing the wafers) and a diffusive flow on the wafer level. When it comes to flow direction over the substrates, this can be further differentiated to parallel (lateral), perpendicular, or stagnant. Reactors handling substrates with a high total surface area can also be operated on a static exposure mode in order to achieve higher precursor utilization efficiency (93).

Commercial ALD reactor systems are typically operated at elevated temperatures. In addition, different types of energy-enhancement sources can be used—especially during the Reactant B step—to lower the thermal budget of the ALD process, which is often a necessity, for example, for applications relying on the handling of sensitive substrates or for processes using thermally unstable reactants. In most of the cases of energy activation, plasma is implemented (either radical enhanced, direct, remote, or a combination of direct and remote plasma) (94), while a few other specialized activations (eg, photo-assisted or hot-wire assisted) have also been reported (11). ALD systems, especially the ones handling wafers, are typically operated under reduced pressure (vacuum to rough vacuum typically between 13 and 1300 Pa). The vacuum, required for the transport and pulsing of the reactants and the purging of the excess reactants and reaction by-products, is created by the use of different types of vacuum pumps, often protected by filters and traps for capturing the highly aggressive reactants or solid particles that would otherwise reduce the equipment's lifetime. Systems delivering higher production volumes are also operated at (near) atmospheric conditions.

Apart from the more conventional approach of temporal separation of the injection and removal of reactants, spatial approaches based on the physical separation of reactants in space have been implemented (95). In that way, (semi)continuous coating of wafers and flexible substrates and also particles/powders has been realized. Especially in the field of particle/powder ALD coating, the intensity of research activities, as illustrated by the number of articles published in scientific journals, has seen an increase over the past years (87). The main focal areas involve applications in the fields of energy storage (96) and catalysis (97). The combination of processing large surface areas with the need for high-volume production has shifted the interest from systems operated in batch mode (eg, fluidized bed reactors) to continuous systems that are often operated at (or near) atmospheric pressure conditions. ALD reactor development is expected to focus on addressing large volume production and processing of a more diverse range of substrate materials. Such an expansion is anticipated to require operation outside the conventional process condition windows, while retaining the high-precision deposition characteristics of ALD coatings. Consequently, a wide range of tailored nanostructured products for a plethora of industrial applications can be enabled.

6. Applications

6.1. Introduction. This section gives an overview of the different commercial applications of ALD. Such information is not easy to retrieve from open sources; it is possible that certain applications that are not made public by the practitioners of the technology will not be covered.

The Soviet-Russian inventors of ALD started developing it based on the framework hypothesis (see Section 2) and soon began to think about possible applications. Since their first substrates were typically silica gels, the first applications they investigated were also powder or particle based: sorbents, catalysts, and rubber fillers. The Finnish inventor started from an application point of view: ALD was developed to obtain better flat panel electroluminescent displays (see Section 2).

ALD has a number of strong points. It is broadly applicable in practice since it couples precision down to subnanometer level, high material quality, and minimum materials usage. It can grow a wide range of materials on many different substrate materials, can be used to coat complex geometries, and can even make structures such as nanolaminates. ALD typically shows good repeatability in different types of equipment and takes place at a relatively low processing temperature (low thermal budget). An additional strong point for commercial application is the good scalability of ALD. First, it is carried out in the gas phase, which industry often prefers over liquid-phase processing, because of, for example, faster processing and absence of solvent waste. Second, while some other coating or deposition techniques rely on beams or directed flows (ie, line-of-sight techniques), ALD just relies on alternating gas concentrations, which is easier to apply at large scale. Finally, many branches of industry prefer continuous processing over batch processing; the current spatial ALD reactors (see Section 5) make that possible too.

ALD has also limitations. It is a slow process, mostly due to the self-terminating reactions and concurrent challenging transport of the reactants. The required precursors are often expensive and/or dangerous due to their high reactivity. The equipment often requires vacuum operation or is otherwise complex. Nevertheless, the commercial use of ALD has strongly increased in recent years.

The most important sector regarding commercial applications of ALD is currently the semiconductor industry. The following sections briefly discuss the commercial applications of ALD that are known in the open literature to be applied in practice.

6.2. Thin-Film Electroluminescent Displays. The reason for Suntola to start the development of ALD was to enable progress in the production of TFEL displays (see Section 2). In 1983, the pilot production of TFEL displays was started by the Finnish company Lohja; they were demonstrated as information boards at the Helsinki-Vantaa airport. The light-emitting layer consisted of ZnS doped with Mn. It takes thousands of cycles to grow, since it is some hundreds of nanometers thick. On both sides of this luminescent layer, a dielectric layer is grown using ALD (see Fig. 21**a**); the high dielectric strength outperformed that of the competing products. While some other companies (Sharp and Planar) had a larger market share than Lohja, the ALD-based product of Lohja was

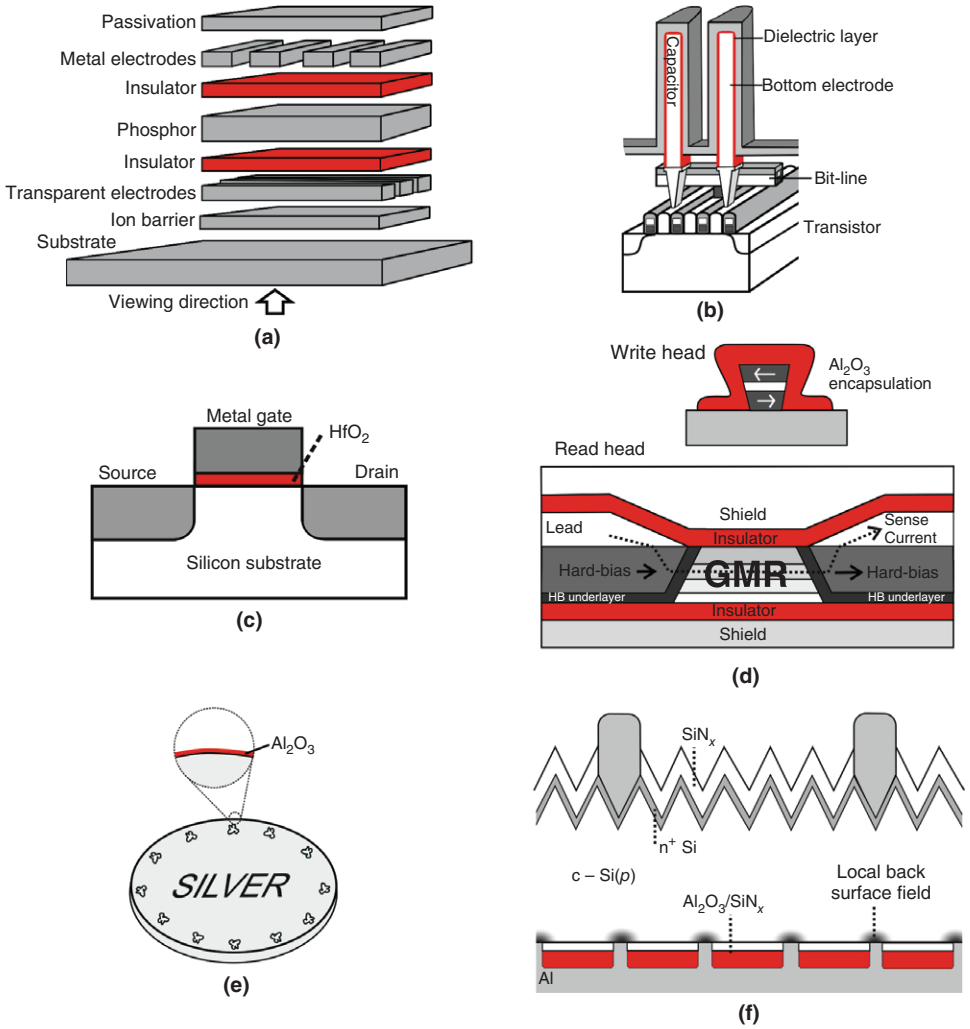

Fig. 21. Schematics of some of the main commercial applications of ALD, with the ALD film given in red: (**a**) TFEL display. Source: Based on Ritala and Leskelä (98); (**b**) 3-D dynamic random access memory. Source: Based on Kim and co-workers (99); (**c**) metal–oxide–semiconductor field-effect transistor; (**d**) write and read head of a hard disk. Source: Based on Williams (100) and Maat and Marley, (101); (**e**) silver coin; (**f**) passivated emitter and reactor contact cell (photovoltaic cell). Source: Based on Macco and co-workers (102). Composite figure source: van Ommen and co-workers (2020), Wikimedia Commons, Creative Commons Attribution 4.0 International license.

superior: the airport information boards at Helsinki-Vantaa airport were used for 15 years continuously, without any element failing (17). Currently, Beneq is marketing TFEL displays under the brand name Lumineq. Most of their models are monochromatic yellow; in some display types multiple colors are used, obtained by filtering the yellow light. TFEL displays are extremely durable and unique in their high transparency but require a high driving voltage (~200 V_{AC}). There are no full-color TFEL displays, since no blue color is available. Up to now, TFEL displays remained a niche product for demanding applications (extreme

temperatures and mechanical shocks), such as on the outside of planes and in industrial operations (17).

6.3. Memory Applications. In the 1990s, it became evident that the continuation of Moore's law (the number of transistors on a microchip doubles roughly every two years) would necessitate the introduction of different architectures, new materials, and novel coating techniques into semiconductor fabrication. This sparked renewed interest in ALD, and ALD—still with the name ALE—entered the International Technology Roadmap for Semiconductors in 2001 (103,104). Large research efforts went into the development of processes to manufacture high-k dielectric materials, metals, and materials for barrier layers (105). High-k dielectric materials for both capacitor dielectrics in Dynamic Random Access Memories (DRAMs) and gate oxides in metal–oxide–semiconductor field effect transistors (MOSFETs) became important topics in ALD research around the year 2000 (106). DRAM became the first major commercial application of ALD in semiconductors.

DRAM is the main memory in modern computers; it is a volatile memory type. The challenge in the shrinking of the size of a DRAM cell (consisting of one capacitor and one transistor) is to keep the capacitance constant (ca 25 fF per cell) (107). A way to follow Moore's law for DRAMs was to move from structures on the silicon substrate (planar) to 3D structures: either beneath the surface (trench) or above the surface (stack). The stack design proved to be the best choice for further steps in decreasing the size: the capacitor structure is made of nanorods perpendicular to the surface with an aspect ratio of ~10–100 (106), see Figure 21**b**. This step—made in the 1990s—also required new materials and led to large-scale industrial implementation of ALD as a deposition method. For processes of 90 nm and lower, high-k materials such as alumina and HfSiON are deposited on the nanorods using ALD (104). Also, other ALD-formed materials, such as ZrO_2–Al_2O_3–ZrO_2 nanolaminates, have been applied (108).

Another important market segment is flash memory. For this nonvolatile memory type, NAND technology (based on logical Not–AND gates) is the most common one. Around 2015, 3D NAND was broadly introduced to enable further growth of memory capacity (109), as further decreasing the size of 2D NAND to follow Moore's law became problematic. A 3D NAND structure typically starts with alternating horizontal layers of SiO_2 and Si_3N_4 (this layer is removed later) in which holes are made using etching. Every crossing of a hole with a retained layer will form a single memory cell, that is, given its functionality by multiple coating steps (eg, depositing a blocking oxide, charge storage layer, tunnel oxide, and transistor channel) (110), of which at least some are typically ALD. As in DRAM, the step to 3D structures favored ALD because of its strength in coating structures with a high aspect ratio (111).

6.4. Metal–Oxide–Semiconductor Field-Effect Transistors. Next to the application in DRAMs, another milestone in the microelectronics industry was the deployment of ALD in microprocessor production. The basic building block of a microprocessor is the MOSFET. The MOSFET has also been scaled down in size over the preceding decades: from several micrometers to tens of nanometers currently. The use of ALD in mass production of microprocessors started with the production of Penryn processors (45 nm technology) in 2007 by Intel (106). Instead of using SiO_2, obtained via thermal oxidation of the Si surface (106), HfO_2

was deposited, using ALD as a high-k dielectric for the transistor gate (12) (see Fig. 21**c**). MOSFETs have stayed for longer than DRAM as planar structures, but from around 2012 the so-called FinFETs (fin field-effect transistors)—a type of MOSFET with structures stacked on the silicon substrate—have been commercialized for 22-nm technology and smaller (112). In FinFETs, ALD has been used to deposit a gate dielectric oxide (eg, HfO_2) and metal gate (eg, TiN) on the side and top walls of the fin structure (106).

6.5. Other Microelectronic Applications. In recent years, ALD has become an important tool in microelectronics. The previous sections already discussed applications in DRAMs, 3D NANDs, and MOSFETs. There are also more generic applications of ALD in microelectronics, such as making self-aligned multiple patterning and area-selective ALD, which will be briefly discussed in this section.

Due to the high costs of extreme ultraviolet lithography for the smallest wavelengths, the semiconductor industry also uses traditional optical lithography combined with multiple patterning techniques to enhance the pattern density. Self-aligned double patterning or spacer lithography is a widely used method (113). In brief, a surface with a pattern of spacers is coated (eg, by ALD) and then etched back: the coating is removed from the top, but not from the side walls. After that, the original spacers are etched away, and the side walls serve as the new spacers. The process can be repeated to go from doubling to quadrupling. Plasma ALD of SiO_2 is widely used for multiple patterning, and its application in the manufacturing of memory and logic devices is a considerable part of the total ALD market (30).

Interconnects, transferring signals between individual components on an integrated circuit, are made during the back-end-of-line processing. Currently, typically Cu interconnects via CVD or PVD are used, but this is approaching the scaling limits. New solutions are typically combination of ALD (eg, TiN and WC as adhesion layer) and CVD (114,115). ALD of alternatives to Cu such as Ni, Co, and Ru is also being investigated (116).

Also, area-selective ALD (see Section 3.7) seems to be at the brink of being applied in the semiconductor industry (117). There are, as far as the authors of this article know, no open reports yet about its industrial application.

6.6. Hard Disk Heads. Around 2000, ALD entered the production of magnetic heads for reading and writing data into hard disks (118). The increased storage capacity of hard disks required all elements to become smaller and smaller. In the 1990s, the giant magnetoresistive (GMR) read head (see Fig. 21**d**) came into use: multilayer structures with layers of a few nanometers thick that could generate bits of much smaller sizes than the earlier used technology (100). When the thickness of the insulation layer, needed for the gap between the read head and the disk, became smaller than 20 nm (~80 GB hard disk, around 2000), the originally used PVD process to make alumina no longer yielded the required conformality. A high breakdown strength and high thermal conductivity, combined with low leakage currents, was required, and the transition to alumina ALD (thermal TMA-water process) was made. The process is not pure ALD; a small CVD component is accepted to boost throughput while maintaining uniformity (119). Around 2006, the critical dimension of the writing head reached a size of 100 nm, and ALD was used to encapsulate it with an insulating alumina layer (see Fig. 21**d**).

The writing head has a trapezoidal shape to avoid erroneously writing data on adjacent tracks (100). ALD thin films and nanolaminates have been investigated and possibly used for other applications in the read/write head process flow, such as trench filling, tunneling barriers, and encapsulation (92). For example, by forming nanolaminates of alumina and silica, an even better insulating layer can be obtained (120).

6.7. Jewelry and Coins. ALD is a good technology for creating a barrier coating, for example, for protecting a metal object against corrosion. In practice, ALD is being applied to protect silver objects against tarnishing (see Fig. 21**e**). Typically ceramic materials such as alumina are applied, with thicknesses around 10 nm. The low thickness is important because it leaves the visual appearance of the silver objects unchanged (118). Multiple commercial companies are involved in such processes: Beneq is, for example, involved in coating silver jewelry (121), and Picosun in coating coins and parts for high-end watches (122,123). During use of these objects the ALD coating might erode rather quickly. This can be an advantage: it enables easier cleaning compared to only partially damaged thick lacquer coatings. Since a thick ALD film would become expensive, one solution would be to combine a thin antitarnishing ALD coating with a thicker antierosion coating when a permanent, erosion-resistant coating is required (118). ALD can also be used for protecting silver artifacts, for example, in museums, but that application is still in the research phase (124). For that application, an additional demand is that the coating can be removed without damage to the object, which is indeed possible using aqueous NaOH.

6.8. Photovoltaic Cells. Around 1990, Suntola and co-workers explored the application of ALD in the production of photovoltaic (PV) cells, but that did not lead to commercial implementation (17). The number of publications on ALD for PV cells started to increase strongly around 2010. Currently, there is a large amount of scientific literature about the role that ALD can play in fabricating PV cells, not only in silicon solar cells but also in, for example, quantum dot and perovskite solar cells. However, the application of ALD in industrial PV processes seems only to originate from recent times; it is not much described in open literature. An important part of the PV cell market is currently taken by the so-called PERC (passivated emitter and rear contact cells). The aluminum contact plate on the back of the cell (the bottom side in Fig. 21**f**) is interrupted by passivation parts to reduce charge carrier recombination, thus enhancing the conversion efficiency (102). Up to recently, plasma-enhanced chemical vapor deposition (PECVD) was the main technology to deposit a thin alumina layer on the passivation parts, but around 2018 ALD started to replace this technology. The better passivation of an alumina coating made by ALD can increase the PV cell efficiency by 0.05% as compared to PECVD. In 2019, most of the large PV cell manufacturers in China—world's main producer of PV cells—were using this technology (125). Since PV cells have a much larger surface area than microchips, the precursor costs are more important. Lin et al. (126) have shown that using solar grade TMA instead of semiconductor grade TMA does not lead to a measurable difference in surface passivation quality. Hence, solar grade TMA—high impurity concentration but cheaper—can safely be used in the PV cell production. Since ALD layer can have more functions than only passivation (eg, creating selective contacts) and can also be very beneficial in emerging PV technologies (eg, thin-film, organic, and

quantum-dot PV cells), a further increase in ALD deployment in the PV market is foreseen (127).

6.9. Miscellaneous. The previous sections have discussed some specific commercial applications of ALD. There are many more potential applications that are being researched and perhaps start to be put in practice. Apart from its use in electronics, ALD is also very well suited for a range of optical applications: ALD coatings are so thin that they hardly interact with photons. For example, in OLED (organic LED) screens, a thin inorganic coating is a way to prevent permeation of oxygen and moisture. The transition from PECVD to ALD in the production of flexible OLED screens has already been announced in 2016 (128), but it remains unclear to what extent this has taken place. There are also various other potential applications of ALD in optics, such as in LED phosphor particles, LED encapsulation, optical sensor, and high-performance mirrors, but the authors of this article are unaware of large-scale deployment at the time of writing.

ALD on powders or particles has already been researched for several decades. Russian researchers already used silica gel in the early stage of ALD investigations. Both Russian and Finnish researchers studied ALD on particles in order to make catalysts (129,130). That work did not directly lead to the production of catalysts using ALD: it was often considered too costly. However, for the current combined production of styrene and propylene oxide, a titanium on silica catalysts is used, which is made by a process that can be considered single-cycle ALD (131). ALD on powders is also widely considered for application in Li-ion batteries, but commercial applications seem not yet widely spread (87). Also, the application in pharmaceutical powders, pigments, and sunscreens is investigated. At the small scale, ALD has been used to produce powder sorbents for, for example, water and organic vapors (132).

Roll-to-roll reactors (see Section 5) can be used to coat plastic foils. This can be used to make packaging materials that are both optically transparent and a very good barrier for oxygen and water (133). However, this is hardly or not applied in practice; probably, it is economically unattractive. Another ALD application is its use in medical implants: a coating can increase the biocompatibility of the implant and give it an antimicrobial function (134,135). However, it is unclear how widespread it is being applied.

7. Conclusions and Outlook

ALD is a chemical method to grow ultrathin layers of materials. It relies on alternatingly exposing a surface to gaseous reactants—separated by a purge step—that react in a self-terminating manner. After its twofold, independent inventions in the 1960s and 1970s, it took multiple decades before ALD's large potential became clear to the international research and industrial community. ALD can be used to grow a large number of materials with high-quality and nanoscale precision. ALD can be applied to many different substrates, even to complex 3D structures. However, it is a slow process, and the required precursors are often expensive and/or dangerous. Contributions from different fields of science and engineering continue to deepen the understanding and broaden the applicability of ALD. Currently, ALD is a commercially important technology in

the semiconductor industry, its market size is strongly growing, and it has the potential to make an impact on several other industrial sectors.

REFERENCES

1. S. E. Thompson and S. Parthasarathy, *Mater. Today* **9**(6), 20–25 (2006). DOI: 10.1016/S1369-7021(06)71539-5
2. C. Mack, *IEEE Spectr.* **52**(4), 31–31 (2015). DOI: 10.1109/MSPEC.2015.7065415
3. V. Miikkulainen and co-workers, *J. Appl. Phys.* **113** (2013). DOI: 10.1063/1.4757907
4. T. Yoshimura, S. Tatsuura, and W. Sotoyama, *Appl. Phys. Lett.* **59**(4), 482–484 (1991). DOI: 10.1063/1.105415
5. S. M. George, *Chem. Rev.* **110**(1), 111–131 (2010). DOI: 10.1021/cr900056b
6. P. Sundberg and M. Karppinen, *Beilstein J. Nanotechnol.* **5**, 1104–1136 (2014). DOI: 10.3762/bjnano.5.123
7. D. J. H. Emslie, P. Chadha, and J. S. Price, *Coord. Chem. Rev.* **257**(23), 3282–3296 (2013). DOI: 10.1016/j.ccr.2013.07.010
8. I. Azpitarte and M. Knez, *MRS Commun.* **8**(3), 727–741 (2018). DOI: 10.1557/mrc.2018.126
9. Y. Wu and co-workers, *Nano Lett.* **15**(10), 6379–6385 (2015). DOI: 10.1021/acs.nanolett.5b01424
10. R. L. Puurunen, *J. Appl. Phys.* **97**(12), 121301 (2005). DOI: 10.1063/1.1940727
11. H. V. Bui, F. Grillo, and J. R. van Ommen, *Chem. Commun.* **53**(1), 45–71 (2017). DOI: 10.1039/C6CC05568K
12. R. W. Johnson, A. Hultqvist, and S. F. Bent, *Mater. Today* **17**(5), 236–246 (2014). DOI: 10.1016/j.mattod.2014.04.026
13. Aalto OpenLearning, Atomic layer deposition – Review articles on ALD. https://openlearning.aalto.fi/course/view.php?id=100&section=4 (accessed 01 December 2020).
14. A. A. Malygin and co-workers, *Chem. Vap. Depos.* **21**(10-11–12), 216–240 (2015). DOI: 10.1002/cvde.201502013
15. T. Suntola and J. Antson, Method for producing compound thin films. U.S. 4,058,430A (Nov. 15, 1977).
16. V. B. Aleskovskii and S. I. Koltsov, in *Abstract of Scientific and Technical Conference of the Leningrad Technological Institute by Lensovet*, Goskhimizdat, Leningrad, 1965, pp. 67–67.
17. R. L. Puurunen, *Chem. Vap. Depos.* **20**(10-11–12), 332–344 (2014). DOI: 10.1002/cvde.201402012
18. S. I. Koltsov, Synthesis of solids by the molecular layering method. Doctor of Science thesis. Leningrad Technological Institute, Leningrad, 1971.
19. T. S. Suntola, A. J. Pakkala, and S. G. Lindfors, Method for performing growth of compound thin films. U.S. 4,413,022A (Nov. 01, 1983).
20. T. Suntola, *Mater. Sci. Rep.* **4**(5), 261–312 (1989). DOI: 10.1016/S0920-2307(89)80006-4
21. R. Paananen (ed.), First Symposium on Atomic Layer Epitaxy. VTT Technical Research Centre of Finland, Espoo, 1984.
22. L. Niinistö (ed.), Proceedings of the First International Symposium on Atomic Layer Epitaxy (ALE-1), Finnish Academy of Technical Sciences, Espoo, 1990.
23. M. Leskela, *Acta Polytech. Scand. Chem. Technol. Ser.* **195**, 67–80 (1990).
24. S. M. George, ed., *1st International Conference on Atomic Layer Deposition*, AVS, Monterey, CA, 2001.

25. V. B. Aleskovskii and V. E. Drozd, *Acta Polytech. Scand. Chem. Technol. Ser.* **195**, 155–161 (1990).
26. J. Aarik, On the mechanism of film formation by ALE from compound sources. Proceedings on electroluminescence. XVIII, Preparation and investigation of thin solid films, Tartu, Estonia, 1990, pp. 47–53, http://hdl.handle.net/10062/32165.
27. VPHA, Virtual Project on the History of ALD. https://www.vph-ald.com/ (accessed 01 December 2020).
28. E. Ahvenniemi and co-workers, *J. Vac. Sci. Technol. A* **35**(1), 010801 (2016). DOI: 10.1116/1.4971389
29. S. E. Potts and W. M. M. Kessels, *Coord. Chem. Rev.* **257**(23), 3254–3270 (2013). DOI: 10.1016/j.ccr.2013.06.015
30. H. C. M. Knoops and co-workers, *J. Vac. Sci. Technol. A* **37**(3), 030902, 10.1116/1.5088582 (2019).
31. IUPAC, Chemisorption (C01048). http://goldbook.iupac.org/terms/view/C01048 (accessed 03 December 2020).
32. T. Blomberg, *ECS Trans.* **58**(10), 3–18 (2013). DOI: 10.1149/05810.0003ecst
33. R. L. Puurunen and W. Vandervorst, *J. Appl. Phys.* **96**(12), 7686–7695 (2004). DOI: 10.1063/1.1810193
34. O. Nilsen and co-workers, *J. Appl. Phys.* **102**(2), 024906 (2007). DOI: 10.1063/1.2756514
35. H. H. Sønsteby, A. Yanguas-Gil, and J. W. Elam, *J. Vac. Sci. Technol. A* **38**(2), 020804 (2020). DOI: 10.1116/1.5140603
36. R. L. Puurunen, *Chem. Vap. Depos.* **9**(5), 249–257 (2003). DOI: https://doi.org/10.1002/cvde.200306265
37. N. E. Richey, C. de Paula, and S. F. Bent, *J. Chem. Phys.* **152**(4), 040902 (2020). DOI: 10.1063/1.5133390
38. S. T. Barry, A. V. Teplyakov, and F. Zaera, *Acc. Chem. Res.* **51**(3), 800–809 (2018). DOI: 10.1021/acs.accounts.8b00012
39. E.-L. Lakomaa, A. Root, and T. Suntola, *Appl. Surf. Sci.* **107**, 107–115 (1996). DOI: 10.1016/S0169-4332(96)00513-2
40. J. Lu and J. W. Elam, *Chem. Mater.* **27**(14), 4950–4956 (2015). DOI: 10.1021/acs.chemmater.5b00818
41. J. Hämäläinen, M. Ritala, and M. Leskelä, *Chem. Mater.* **26**(1), 786–801 (2014). DOI: 10.1021/cm402221y
42. L. Nyns and co-workers, *ECS Trans.* **16**(4), 257–267 (2008). DOI: 10.1149/1.2980001
43. R. L. Puurunen, *Chem. Vap. Depos.* **9**(6), 327–332 (2003). DOI: https://doi.org/10.1002/cvde.200306266
44. R. L. Puurunen, *Appl. Surf. Sci.* **245**(1), 6–10 (2005). DOI: 10.1016/j.apsusc.2004.10.003
45. T. Hatanpää, M. Ritala, and M. Leskelä, *Coord. Chem. Rev.* **257**(23), 3297–3322 (2013). DOI: 10.1016/j.ccr.2013.07.002
46. E.-L. Lakomaa, *Appl. Surf. Sci.* **75**(1), 185–196 (1994). DOI: 10.1016/0169-4332(94)90158-9
47. R. L. Puurunen and co-workers, *Appl. Phys. Lett.* **86**(7), 073116 (2005). DOI: 10.1063/1.1866219
48. F. Grillo and co-workers, *J. Phys. Chem. Lett.* **8**(5), 975–983 (2017). DOI: 10.1021/acs.jpclett.6b02978
49. J. Dendooven and co-workers, *Nat. Commun.* **8**(1), 1 (2017). DOI: 10.1038/s41467-017-01140-z
50. R. L. Puurunen, *Chem. Vap. Depos.* **10**(3), 159–170 (2004). DOI: https://doi.org/10.1002/cvde.200306283
51. R. L. Puurunen and co-workers, *J. Appl. Phys.* **96**(9), 4878–4889 (2004). DOI: 10.1063/1.1787624

52. A. J. M. Mackus, M. J. M. Merkx, and W. M. M. Kessels, *Chem. Mater.* **31**(1), 2–12 (2019). DOI: 10.1021/acs.chemmater.8b03454
53. G. N. Parsons and R. D. Clark, *Chem. Mater.* **32**(12), 4920–4953 (2020). DOI: 10.1021/acs.chemmater.0c00722
54. A. Yanguas-Gil, *Growth and Transport in Nanostructured Materials: Reactive Transport in PVD, CVD, and ALD*, Springer International Publishing, Cham, 2017.
55. V. Cremers, R. L. Puurunen, and J. Dendooven, *Appl. Phys. Rev.* **6**(2), 021302 (2019). DOI: 10.1063/1.5060967
56. K. Arts and co-workers, *J. Phys. Chem. C* **123**(44), 27030–27035 (2019). DOI: 10.1021/acs.jpcc.9b08176
57. P. Poodt and co-workers, *J. Vac. Sci. Technol. A* **35**(2), 021502 (2017). DOI: 10.1116/1.4973350
58. J. Yim and co-workers, *Phys. Chem. Chem. Phys.* **22**(40), 23107–23120 (2020). DOI: 10.1039/D0CP03358H
59. M. Ylilammi, O. M. E. Ylivaara, and R. L. Puurunen, *J. Appl. Phys.* **123**(20), 205301 (2018). DOI: 10.1063/1.5028178
60. K.-E. Elers and co-workers, *Chem. Vap. Depos.* **12**(1), 13–24 (2006). DOI: https://doi.org/10.1002/cvde.200500024
61. J. W. Elam and co-workers, *Thin Solid Films* **436**(2), 145–156 (2003). DOI: 10.1016/S0040-6090(03)00533-9
62. H. H. Sønsteby and co-workers, *Chem. Mater.* **30**(3), 1095–1101 (2018). DOI: 10.1021/acs.chemmater.7b05005
63. J. Aarik and co-workers, *Appl. Surf. Sci.* **103**(4), 331–341 (1996). DOI: 10.1016/S0169-4332(96)00554-5
64. A. B. Mukhopadhyay and C. B. Musgrave, *Chem. Phys. Lett.* **421**(1), 215–220 (2006). DOI: 10.1016/j.cplett.2006.01.057
65. J. W. Elam and S. M. George, *Chem. Mater.* **15**(4), 1020–1028 (2003). DOI: 10.1021/cm020607+
66. K. J. Kanarik and co-workers, *J. Vac. Sci. Technol. A* **33**(2), 020802 (2015). DOI: 10.1116/1.4913379
67. S. M. George, *Acc. Chem. Res.* **53**(6), 1151–1160 (2020). DOI: 10.1021/acs.accounts.0c00084
68. T. Aaltonen, Atomic layer deposition of noble metal thin films. PhD thesis. University of Helsinki, Helsinki, 2005.
69. M. Ritala and co-workers, *Science* **288**(5464), 319–321 (2000). DOI: 10.1126/science.288.5464.319
70. S. García-García and co-workers, *Chem. Sci.* **10**(7), 2171–2178 (2019). DOI: 10.1039/C8SC04474K
71. M. D. Losego and Q. Peng, in *Surface Modification of Polymers*, New York, John Wiley & Sons, Inc., 2019, pp. 135–159.
72. D. Hausmann and co-workers, *Science* **298**(5592), 402–406 (2002). DOI: 10.1126/science.1073552
73. O.-K. Kwon and co-workers, *J. Electrochem. Soc.* **151**(2), G109–G112 (2004). DOI: 10.1149/1.1640633
74. M. Mattinen and co-workers, *Langmuir* **32**(41), 10559–10569 (2016). DOI: 10.1021/acs.langmuir.6b03007
75. R. Matero and co-workers, *Thin Solid Films* **368**(1), 1–7 (2000). DOI: 10.1016/S0040-6090(00)00890-7
76. F. Grillo and co-workers, *Small* **14**(23), 1800765 (2018). DOI: 10.1002/smll.201800765
77. H. C. M. Knoops, S. E. Potts, A. A. Bol, and W. M. M. Kessels, in T. F. Kuech, ed. *Handbook of Crystal Growth*, 2nd ed., Boston, MA, North-Holland, 2015, pp. 1101–1134.
78. T. Hatanpää and co-workers, *Dalton Trans.* **39**(13), 3219–3226 (2010). DOI: 10.1039/B918175J

79. J. Niinistö and co-workers, *ECS Trans.* **64**(9), 221232 (2014). DOI: 10.1149/06409.0221ecst
80. A. L. Egorov and Y. K. Ezhovskii, *J. Appl. Chem. USSR* **57**(4), 685–688 (1984). https://scholar.google.com/scholar_lookup?hl=en&volume=57&publication_year=1984&pages=738&author=A.+L.+Egorovauthor=Yu.+K.+Ezhovskii&title=Preparation+of+ultra+thin+silicon+dioxide+films+on+the+tantalum+surface+by+the+chemical+buildup+method (accessed 21 March 2021)
81. J. W. Klaus, O. Sneh, and S. M. George, *Science* **278**(5345), 1934–1936 (1997). DOI: 10.1126/science.278.5345.1934
82. V. V. Brei, V. A. Kaspersky, and N. U. Gulyanitskaya, *React. Kinet. Catal. Lett.* **50**(1–2), 415–421 (1993).
83. J. M. Lownsbury and co-workers, *Chem. Mater.* **29**(20), 8566–8577 (2017). DOI: 10.1021/acs.chemmater.7b01491
84. A. Delabie and co-workers, *J. Appl. Phys.* **97**(6), 064104 (2005). DOI: 10.1063/1.1856221
85. T. Aaltonen and co-workers, *Chem. Mater.* **15**(9), 1924–1928 (2003). DOI: 10.1021/cm021333t
86. J. Dendooven and co-workers, *J. Phys. Chem. C* **117**(40), 20557–20561 (2013). DOI: 10.1021/jp403455a
87. J. R. van Ommen and A. Goulas, *Mater. Today Chem.* **14**, 100183 (2019). DOI: 10.1016/j.mtchem.2019.08.002
88. H.-C. Yang and co-workers, *Nanoscale* **10**(44), 20505–20513 (2018). DOI: 10.1039/C8NR08114J
89. P. Poodt and co-workers, *J. Vac. Sci. Technol. A* **30**(1), 010802 (2011). DOI: 10.1116/1.3670745
90. S. Chu, in C. S. Hwang, ed. *Atomic Layer Deposition for Semiconductors*, Boston, MA, Springer US, 2014, pp. 241–255.
91. P. O. Oviroh and co-workers, *Sci. Technol. Adv. Mater.* **20**(1), 465–496 (2019). DOI: 10.1080/14686996.2019.1599694
92. A. Pakkala and M. Putkonen, in P. M. Martin, ed. *Handbook of Deposition Technologies for Films and Coatings (Third Edition)*, Boston, MA, William Andrew Publishing, 2010, pp. 364–391.
93. J. A. McCormick and co-workers, *J. Vac. Sci. Technol. A* **25**(1), 67–74 (2007). DOI: 10.1116/1.2393299
94. H. B. Profijt and co-workers, *J. Vac. Sci. Technol. A* **29**(5), 050801 (2011). DOI: 10.1116/1.3609974
95. P. Poodt and co-workers, *J. Vac. Sci. Technol. A* **31**(1), 01A108 (2012). DOI: 10.1116/1.4756692
96. L. Ma and co-workers, *Adv. Mater. Interfaces* **3**(21), 1600564 (2016). DOI: 10.1002/admi.201600564
97. R. K. Ramachandran, C. Detavernier, and J. Dendooven, in *Nanotechnology in Catalysis*, New York, John Wiley & Sons, Inc., 2017, pp. 335–358.
98. M. Ritala and M. Leskelä, in H. Singh Nalwa, ed. *Handbook of Thin Films*, Burlington, Academic Press, 2002, pp. 103–159.
99. S. K. Kim and co-workers, *Adv. Funct. Mater.* **20**(18), 2989–3003 (2010). DOI: 10.1002/adfm.201000599
100. K. E. Williams, *Solid State Technol.* **47**(9), S21–S21 (2004).
101. S. Maat and A. C. Marley, in Y. Xu, D. D. Awschalom, and J. Nitta, eds. *Handbook of Spintronics*, Dordrecht, Springer Netherlands, 2016, pp. 977–1028.
102. B. Macco, B. W. van de Loo, and W. M. Kessels, in *Atomic Layer Deposition in Energy Conversion Applications*, New York, John Wiley & Sons, Inc., 2017, pp. 41–99.

103. Front End Processes, International Technology Roadmap for Semiconductors 2001 Edition. https://www.semiconductors.org/wp-content/uploads/2018/08/2001FEP.pdf (accessed 18 December 2020).
104. ITRS Reports International Technology Roadmap for Semiconductors. http://www.itrs2.net/itrs-reports.html (accessed 18 December 2020).
105. Front End Processes, International Technology Roadmap for Semiconductors 2003 Edition. https://www.semiconductors.org/wp-content/uploads/2018/08/FEP2003.pdf (accessed 18 December 2020).
106. C. S. Hwang, ed., *Atomic Layer Deposition for Semiconductors*, Springer US, Boston, MA, 2014.
107. K. H. Kuesters and co-workers, *Adv. Eng. Mater.* **11**(4), 241–248 (2009). DOI: 10.1002/adem.200800298
108. M. Leskelä, M. Ritala, and O. Nilsen, *MRS Bull.* **36**(11), 877–884 (2011). DOI: 10.1557/mrs.2011.240
109. J. H. Yoon and co-workers, *Flash Mem. Summit* **3**(4.2), 3–4 (2017).
110. C. Petti, 3D memory: Etch is the new litho. Advanced Etch Technology for Nanopatterning VII, March 2018, vol. 10589, 1058904. DOI: 10.1117/12.2297131.
111. S. Ver-Bruggen, *Solid State Technol.* **57**(2), 34–38 (2014). https://jglobal.jst.go.jp/en/detail?JGLOBAL_ID=201402200069336770 (accessed 27 November 2020)
112. D. James, Intel Ivy Bridge unveiled—The first commercial tri-gate, high-k, metal-gate CPU. Proceedings of the IEEE 2012 Custom Integrated Circuits Conference, 2012. DOI: 10.1109/CICC.2012.6330644.
113. B. Chang, *J. Vac. Sci. Technol. B* **38**(3), 032601 (2020). DOI: 10.1116/6.0000089
114. F. Griggio, J. Palmer, F. Pan, N. Toledo, and A. Schmitz, Reliability of dual-damascene local interconnects featuring cobalt on 10 nm logic technology. 2018 IEEE International Reliability Physics Symposium (IRPS), 2018, p. 6E.3-1–6E.3–5. DOI: 10.1109/IRPS.2018.8353641.
115. M. Lapedus, New BEOL/MOL breakthroughs? Semiconductor Engineering, 2017. https://semiengineering.com/new-beolmol-breakthroughs/ (accessed 18 December 2020).
116. K. Väyrynen, Atomic layer deposition of late first-row transition metals : precursors and processes. PhD thesis, University of Helsinki, 2019.
117. H.-B.-R. Lee and S. F. Bent, *Chem. Mater.* **32**(8), 3323–3324 (2020). DOI: 10.1021/acs.chemmater.0c00838
118. M. Ritala and J. Niinistö, *ECS Trans.* **25**(8), 641–652 (2009). DOI: 10.1149/1.3207651
119. M. Kautzky and co-workers., Applications of atomic layer deposition in magnetic recording heads. Presented at the AVS 3rd International Conference on Atomic Layer Deposition, San Jose, 2003.
120. M. Mao, R. Bubber, and T. Schneider, *ECS Trans.* **1**(10), 37–47 (2006). DOI: 10.1149/1.2209328
121. Beneq, Anti-tarnishing coating for jewelry, 2020. https://beneq.com/en/success-story/anti-tarnishing-coating-for-jewelry/ (accessed 20 December 2020).
122. Picosun, Picosun's ALD technology protects coins, 2013. http://www.picosun.com/press/picosuns-ald-technology-protects-coins/ (accessed 20 December 2020).
123. Picosun, Picosun's ALD solutions make quality watches tick, 2018. https://www.picosun.com/press/picosuns-ald-solutions-make-quality-watches-tick/ (accessed 20 December 2020).
124. E. Breitung and co-workers., Multi-layer protective coatings on silver for protection of historic silver artifacts. Presented at the AVS 19th International Conference on Atomic Layer Deposition (ALD 2019), Bellevue, 2019.
125. B. O'Donnell, Atomic layer deposition storms market for PERC. pv magazine International. https://www.pv-magazine.com/2019/06/29/the-weekend-read-atomic-layer-deposition-storms-market-for-perc/ (accessed 11 December 2020).

126. F. Lin, N. Nandakumar, B. Dielissen, R. Görtzen, and B. Hoex, Excellent surface passivation of silicon at low cost: atomic layer deposited aluminium oxide from solar grade TMA. 2013 IEEE 39th Photovoltaic Specialists Conference (PVSC), June 2013, pp. 1268–1271. DOI: 10.1109/PVSC.2013.6744372
127. M. A. Hossain and co-workers, *Nano Mater. Sci.* **2**(3), 204–226 (2020). DOI: 10.1016/j.nanoms.2019.10.001
128. ETNEWS, Korea IT News, Samsung and LG planning to apply ALD technology into flexible OLED. 23 September 2016. www.etnews.com. https://english.etnews.com/20160923200003?SNS=00002 (accessed 29 November 2020).
129. S. I. Koltsov, V. M. Smirnov, and V. B. Aleskovskii, *Kinet. Catal.* **11**, 835–841 (1970).
130. M. Lindblad, L. P. Lindfors, and T. Suntola, *Catal. Lett.* **27**(3), 323–336 (1994). DOI: 10.1007/BF00813919
131. J. K. F. Buijink and co-workers, *Catal. Today* **93–95**, 199–204 (2004). DOI: 10.1016/j.cattod.2004.06.041
132. A. A. Malygin, *Bull. St. Petersburg State Inst. Technol. Tech. Univ.* **1**, 061–067 (2013).
133. T. Hirvikorpi and co-workers, *Thin Solid Films* **550**, 164–169 (2014). DOI: 10.1016/j.tsf.2013.10.148
134. L. Liu, R. Bhatia, and T. J. Webster, *Int. J. Nanomed.* **12**, 8711–8723 (2017). DOI: 10.2147/IJN.S148065
135. A. A. Solovyev and co-workers, *Eur. Cell. Mater.* **27**(2), 17 (2014).

J. Ruud van Ommen
Aristeidis Goulas
Delft University of Technology, Faculty of Applied Sciences, Department of Chemical Engineering, Delft, The Netherlands

Riikka L. Puurunen
Aalto University, School of Chemical Engineering, Department of Chemical and Metallurgical Engineering, Aalto, Finland